Accepted Manuscript

Development of a series of novel 4-anlinoquinazoline derivatives possessing quinazoline skeleton: Design, synthesis, EGFR kinase inhibitory efficacy, and evaluation of anticancer activities *in vitro*

Jin Chang, Hongyu Ren, Mingxia Zhao, Yan Chong, Wenwen Zhao, Yong He, Yunling Zhao, Huabei Zhang, Chuanmin Qi

PII: S0223-5234(17)30527-5

DOI: 10.1016/j.ejmech.2017.07.005

Reference: EJMECH 9568

To appear in: *European Journal of Medicinal Chemistry*

Received Date: 30 August 2016

Revised Date: 1 July 2017

Accepted Date: 3 July 2017

Please cite this article as: J. Chang, H. Ren, M. Zhao, Y. Chong, W. Zhao, Y. He, Y. Zhao, H. Zhang, C. Qi, Development of a series of novel 4-anlinoquinazoline derivatives possessing quinazoline skeleton: Design, synthesis, EGFR kinase inhibitory efficacy, and evaluation of anticancer activities *in vitro*, *European Journal of Medicinal Chemistry* (2017), doi: 10.1016/j.ejmech.2017.07.005.

This is a PDF file of an unedited manuscript that has been accepted for publication. As a service to our customers we are providing this early version of the manuscript. The manuscript will undergo copyediting, typesetting, and review of the resulting proof before it is published in its final form. Please note that during the production process errors may be discovered which could affect the content, and all legal disclaimers that apply to the journal pertain.

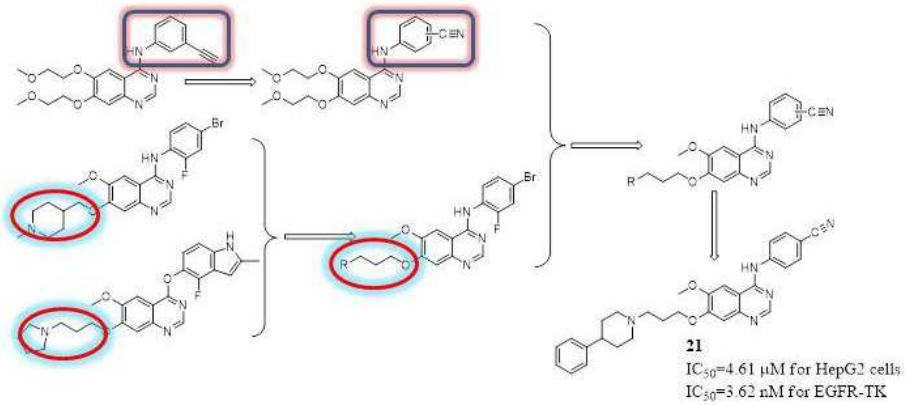

21
IC_{50}=4.61 μM for HepG2 cells
IC_{50}=3.62 nM for EGFR-TK

ACCEPTED MANUSCRIPT

ACCEPTED MANUSCRIPT

Development of a series of novel 4-anlinoquinazoline derivatives possessing quinazoline skeleton: Design, synthesis, EGFR kinase inhibitory efficacy, and evaluation of anticancer activities *in vitro*

Jin Chang[†], Hongyu Ren[†], Mingxia Zhao[§], Yan Chong[†], Wenwen Zhao[†], Yong He[‡], Yunling Zhao[‡], Huabei Zhang[†], Chuanmin Qi[†, *]

[†]Key Laboratory of Radiopharmaceuticals, Ministry of Education, College of Chemistry, Beijing Normal University, Beijing, 100875, P. R. China.

[‡]Experimental Chemistry Center, College of Chemistry, Beijing Normal University, Beijing Normal University, Beijing, 100875, P. R. China.

[§]Shanxi Institute of Technology, Yangquan, Shanxi, 045000, P. R. China.

Corresponding Author:

*To whom correspondence should be addressed: Phone: +86-13681380097, Fax: +86-10-58802075. E-mail: qicmin@sohu.com

ACCEPTED MANUSCRIPT

ABSTRACT

4-anilinoquinazoline-based derivatives represent an attractive scaffold for small molecular EGFR-TKIs in the field of medicinal chemistry. A series of novel heterocyclic substituted derivatives have been designed, synthesized and evaluated their antitumor bioactivities as potential EGFR-TKIs. Most of the new compounds exhibited certain efficient inhibition potency for proliferation of a panel of five human cancer cells with IC_{50} values at the low micromolar level, and some of them possessed good broad-spectrum inhibition activities, compared to Gefitinib. Especially, the IC_{50} values of compound **21** against HepG2, A549, MCF-7, DU145 and SH-SY5Y cells were 4.61, 9.50, 9.80, 6.79 and 7.77 μM, respectively, which were much lower than those of Gefitinb. Furthermore, the highlighting compound **21** demonstrated excellent inhibition activity against EGFR-TK with the IC_{50} value of 3.62 nM, similar to that of Gefitinib(2.21 nM). The results of LDH release assay proved that compound **21** was anti-proliferative rather than cytotoxicity on HepG2 cells. Compound **21** were able to cause HepG2 cells to block in S phase and induce cell death mainly by apoptosis through a mitochondrial dependent pathway. Moreover, the assessment of MMP, the determination of intracellular free Ca^{2+} concentration, the production of ROS, and the effects on the activity of caspase-3 in a dose-dependent manner demonstrated that compound **21** induced cell apoptosis in HepG2 cells through the Ca^{2+}/ROS-mediated mitochondria/caspase-dependent apoptosis pathway largely. These preliminary results evidenced that compound **21** could be a potential antitumor agent deserving further study.

Key Words: 4-anilinoquinazoline derivatives; antitumor; anti-proliferative;

EGFR-TK inhibitory; cell cycle; cell apoptosis; mechanism of apoptosis

1. Introduction

Malignant tumor, also called cancer, is consider to be one of the most difficult to cure diseases around the world today [1]. Surgery, radiotherapy and chemotherapy are three major options for the cancer treatment up to present. Chemotherapy drugs provide a unique method for systemic treatment of cancer [2, 3]. A major challenge for antitumor drugs is to design new drugs that will more selectively inhibit cancer cells in order to avoid undesirable side effects on normal cells. Targeted cancer therapies may be more effective than other types of current treatments, due to less harmful to normal cells and more safe and efficient than conventional cytotoxic chemotherapies [4, 5]. Molecular targets for selective inhibitors that play pivotal roles in the initiation and development of tumors may obtain the greatest clinical benefit with minimal side effects [6, 7]. Protein tyrosine kinases (PTKs) are involved in the regulation of almost all major cellular functions, such as cell proliferation, growth, metabolism, survival, differentiation and apoptosis [8-10]. Several PTKs are known to be activated in response to many tumor cell growth factors extensively and facilitate tumor growth and progression, which have emerged as a new potential and effective therapeutic approach in antitumor therapy. Hence, tumor growth inhibition (TGI) by

directly targeting RTKs without side effects may provide an attractive new strategy for cancer chemotherapy.

The epidermal growth factor receptor (EGFR) functions in mediating proliferation, differentiation, and survival of normal as well as tumor cells. EGFR over-expression or over-activity have been associated with many tumor types, including non-small cell lung, breast, ovarian and squamous cell cancers, leading to uncontrolled proliferation and insensitivity to apoptotic stimuli [11-14]. Most targeted drug therapies extensively explored in clinical trials are either small molecule tyrosine kinase inhibitors or monoclonal antibodies. Small molecule EGFR-TKIs have become a major molecular target for selective anticancer drugs with a much lower risk of side effects[15, 16]. The most potential small molecule selective EGFR-TKIs are derived from currently three series of organic small molecules, which include 4-anilinoquinazoline derivatives, 4-[ar(alk)ylamino]pyridopyrimidine derivatives and 4-phenylaminopyrrolopyrimidine derivatives[3]. Most of the 4-anilinoquinazoline-type compounds including the marketing of antitumor agents such as Gefitinib, Erlotinib，Lapatinib and Vandetanib etc.(**Fig. 1**) have been shown to produce clinical therapeutic benefit against a variety of tumors. Numerous 4-anilinoquinazoline TKIs also have been described in the published literature and generally exhibit potent inhibitory activities *in vitro* at nanomolar concentrations[17]. The co-crystal structures of EGFR-TK with Gefitinib and Erlotinib have provided a rich set of structural information for drug discovery efforts on EGFR-TKIs. The ATP binding modes of these EGFR-TKIs have been mostly well elucidated [18, 19]. The binding mode analysis of Gefitinib indicates several key interactions with the ATP pocket of EGFR, None of the X-ray studies have indicated that the amine function at C-4 is involved in binding. The solvent region generally tolerates a variety of polar functional groups without affecting the efficacy too much. Changes and modifications of side chains in the solvent zone can alter and influence the physicochemical properties of the inhibitors[14].

Fig. 1

Inspired by the great potential and importance of these compounds, much attention has been paid to the design and synthesis of novel 4-anilinoquinazoline derivatives and/or functionalized derivatives. More recently, we have previously reported the synthesis of a series of novel quinazoline nitrogen mustard derivatives, and their potential antitumor activities. Studies on molecular mechanisms demonstrated that it can induce the S phase cell cycle arrest and cell apoptosis in HepG2 cells[20]. To enhance EGFR targeted therapies and ameliorate drug properties, side chain modification at C-6 and/or C-7 of the quinazoline scaffold may be able to improve physic-chemical properties and offer a more beneficial pharmacokinetic profile. In the present research, our purpose was to utilize the quinazoline as skeleton for construction of EGFR-TKIs, as part of our follow-up drug research effort to explore the optimal alkyl substitution at the C-7 position, the substituents present at the

fragment of the heterocycle, often called solubilizing tail, are directed to the entrance of the ATP binding site. We have designed and synthesized a novel series of 4-anilinoquinazoline substituted compounds containing different water-solubilizing groups to help improving the pharmacokinetic properties of these inhibitors and evaluated their anti-proliferative against a panel of five human cancer cell lines of different types by MTT assay as well as EGFR-TK inhibition activities by ELISA assay. And then we further have studied the mechanism of inhibiting tumor growth and inducing apoptosis of cancer cells.

2. Results and discussion

2.1. Chemistry

To discover and develop suitable small molecular ATP-competitive EGFR-TKIs as potential anticancer drugs containing the 4-anilinoquinazoline pharmacophore for the tumor treatment of selective targeting, based on the structure-activity relationships(SAR) or quantitative structure-activity relationships(QSAR) of the 4-anilinoquinazolines reported previously, and forasmuch as Vandetanib and Cediranib as lead compounds, we have modified the quinazoline core by using various substituents at C-7 position or C-4 position and designed a series of novel analogues: replacement of the benzene ring at C-4 position with cyanobenzene, retaining methoxy group at C-6 position and introduction of heterocycle-substituted propoxy side chain at C-7 position of the quinazoline nucleus to determine whether these derivatives possess greater inhibition of cell proliferation and higher induction of cell apoptosis.

In order to synthesize all target compounds, we used commercially available compound as the starting materials as outlined in **Scheme 1**[21, 22]. The general process is depicted as follows: Methyl vanillate **1** was selected as the starting material for the preparation of intermediate compounds **2-5** by alkylation, nitration, catalytic hydrogenation, cyclization, respectively. Compound **5** was reacted with phosphorus oxychloride to obtain the key intermediate 4-chloroquinazolines **6**. The compounds **7a-c** was synthesized using the intermediate **6** with different substituted anilines. The final products **8-41** were obtained by reaction of **7a-c** with different aliphatic amines in high yields. All the target compounds are listed in **Table 1**.

Scheme 1

Table 1

2.2. Biological evaluation

2.2.1. *In vitro* anti-proliferative activity screening of target compounds

It is accepted wisdom that cellular evaluations of RTK inhibitory activities provide

more meaningful results for *in vivo* studies than direct measurements of enzyme activity. The antitumor drug discovery screen *in vitro* has been designed to distinguish between broad-spectrum antitumor and selective antitumor agents. In a first screening, the target compounds were screened for the anti-proliferative activities against a panel of five human cancer cell lines, belonging to different tumor types, namely human liver cancer cell lines (HepG2), human lung carcinoma cell lines (A549), human breast carcinoma cell lines (MCF-7), human prostate cancer cell lines (DU145) and human neuroblastoma cell lines (SH-SY5Y) at a concentration of 0.1-100 μM. Gefitinib and QWL-22b(our group have reported) were used as positive control drugs. All the compounds were investigated for their anti-proliferative activities *in vitro* by the MTT assay after 72 h. The inhibitory activities (IC_{50} values) are summarized in **Table 2**. The IC_{50} values that were higher than 100 μM in all cell lines were not included.

Table 2

As depicted in **Table 2**, the cellular results indicated that most of the active analogs exhibited distinctive potential selective or broad-spectrum antitumor activities in five cancer cell lines (*viz*. NCI, Merryland, USA) by introduction of aminoalkyl at C-7 position of quinazoline nucleus, however, compounds **12**, **13**, **19** and **22** were totally inactive. Concerning selectivity against individual cancer cell line, most of the compounds showed effectiveness against HepG2 cells, displaying IC_{50} values range of 0.77 to 29.50 μM compared to Gefitinib and QWL-22b (29.79 and 3.06 μM, respectively). Compounds **21**, **24**, **26**, **29**, **38** and **40** were found to possess significant anti-proliferative activity against HepG2 cells with IC_{50} values of 4.61, 8.84, 9.58, 0.77, 4.03 and 2.11 μM, respectively. Similarly, most of the compounds overall inhibited the growth of SH-SY5Y cells with IC_{50} values ranging from 5.44 to 28.92 μM in comparison with Gefitinib and QWL-22b (18.21 and 8.60 μM, respectively). Compounds **14**, **16**, **21**, **24**, **26**, **32**, **33** and **34** showed higher anti-proliferative activities with IC_{50} values of 8.08, 7.90, 7.77, 9.81, 5.44, 7.33, 6.89 and 6.27 μM, respectively. Interestingly, compound **27** significantly and selectively inhibited the growth of A549 cells with IC_{50} value of 9.82 μM, which was superior to Gefitinib(12.08 μM).

Meanwhile, with regard to broad-spectrum antitumor activity, the results revealed that the active compounds **21** and **40** have effective growth inhibition of all cancer lines in the preliminary screening. Compound **21** displayed the strong and broad-spectrum anti-proliferative activities against various types of cell lines with IC_{50} values range of 4.61 to 9.80 μM, which were relatively higher than those of Gefitinib. Besides, compound **40** showed evident activities against various different cell lines with IC_{50} values range of 2.11 to 9.07 μM.

As mentioned above, compound **21** exhibited broad-spectrum potent antitumor activities against the tested five human cancer cell lines. We further evaluated compound **21** as potential antitumor drug. The MTT method was applied to further

detect the anti-proliferation activities of compound **21** against HepG2 cells and A549 cells *in vitro*. The results of the effects of treatment time- and dosage-dependent on cell lines were showed in **Tables 3, 4** and **Figs. 2, 3**. It was found that compound **21** exerted antitumor effects in a time- and dosage-dependent manner and the IC_{50} values of **21** were 13.02, 9.56 and 5.29 μM after 24, 48 and 72 h, respectively. Significant differences between groups were considered statistically significant at $^{*}P < 0.05$.

Table 3 and Table 4

Fig. 2 and Fig. 3

As can be seen in **Table 5**, compound **21** treatment at less than 10 μM for 48 h on HepG2 cells and less than 10 μM for 72 h on A549 cells began to exhibit significant inhibition effect compared with control, and the inhibition activity increased with the increasing treatment time and dosage of target compound which was confirmed by synchronous morphological observation. On the basis of these results, compound **21** was chosen according to the distinctive effect for further biological studies, including LDH activities assay, cell cycle analysis, cell apoptosis induction, and fluorescence image assay in order to reveal a more detailed picture on the possible anti-proliferative and cell apoptosis induction mechanisms. Significant differences between groups were considered statistically significant at $^{*}P < 0.05$.

Table 5

The excellent results obtained from compound **21** against human cancer cells prompted us to study the selectivity on human normal cell lines and cancer cell lines to evaluate the toxic side effects. The anti-proliferative effects of compound **21** were evaluated on CCC-HPF-1 cells and A549 cells using standard cell viability protocol. As described in **Table 6**, there was excellent selectivity in cell viability with IC_{50} values of 27.97 and 9.50 μM, respectively, which were similar to those of Gefitinib (30.78 and 14.08 μM, respectively). Generally, it was evident compound **21** showed selective anti-proliferative activities on human normal cells and cancer cells to some extent. Significant differences between groups were considered statistically significant at $^{*}P < 0.05$.

Table 6

2.2.2. Structure-activity relationships and molecular docking

The changes of biological activities of the tested compounds could be correlated to

the structure variations and/or modifications. Some general trends concerning structure-activity relationships observed from the results on the title compounds are as follows: With the introduction of a substitution at position 7- in the quinazoline skeleton, we did obtain some active derivatives even if the IC_{50} values against five tested cancer cells were much higher than those of Gefitinib. In particular, the derivatives bearing a 4-phenyl-piperidinyl, 4-piperidinyl-piperidinyl, 4-ethyl-piperazinyl, and pyrrolyl in C-7 position quinazoline ring linked by propyl side chain resulted the higher anti-proliferative activities on HepG2 cells. The introduction of a cyano amino group at C-4 position quinazoline core led to some compounds with IC_{50} values on HepG2 cells lower than those of Gefitinib. However, no significant increase in the anti-proliferative activities was observed from compounds **12**, **13**, **19** and **22** by introducing of methylbenzylamino, hydroxyethylbenzylamino, 2-hydroxyethyl-piperidinyl and tetrahydroisoquinolyl group in C-7 position quinazoline ring linked by propyl side chain respectively exhibited greater reduction in the inhibitory activity. It may be due to the rigidity of the benzene ring and the steric hindrance of the substituents. Compounds **17** and **18** bearing 4-hydroxypiperidinyl and 4-hydroxyethylpiperidinyl group at R_2, exhibited significant decrease in the anti-proliferative activities (IC_{50} values ranging from 21.62 μM to more than 100 μM toward HepG2 cells), which might be induced by the electro-negativity of the oxygen atoms by our conjecture.

To explain the function of the 4-amino group in protein-ligand binding, the size and electronic properties of substituent have been varied by cyano group. Moreover, modifications of substituent position might reveal favorable interactions and size restrictions in this part of the binding pocket. The test results were summarized in **Table 2**. The initial plan to improve potency was to scan for possible hydrogen bonding interactions and lipophilic contacts. Substituents varied in the 4-amino group linked cyano group were to seek for possible lipophilic contacts. As compared to Gefitinib, the potency of inhibitory activities against HepG2 cells was increased from 29.79 to 2.11 μM by introducing a cyano group including para-, meta- and ortho-substituents in aniline ring. Compounds **26**, **34** and **40** with cyano substituent at different position showed distinct inhibitory activity against HepG2 cells. Compound **40** with ortho-cyano substituent showed more potent activity (IC_{50} = 2.11 μM) than compound **26** with para-cyano substituent (IC_{50} = 9.58 μM). The activity of the latter was higher than compound **34** with meta-cyano substituent (IC_{50} = 13.69 μM). The results suggested that substituents in different positions led to different inhibitory activities. This rule was also found in other substituted compounds. It also demonstrated that introduction of certain substituents at para- or ortho- position is more favorable than at meta- position. It may be related to whether it is more beneficial to form a hydrogen bond with the amino acid residues of the skeleton of the hydrophobic cavity. All the above SARs were also suitable for the inhibitory activities of these compounds against A549 cells. However, the inhibitory activities against A549 cells were much weaker than those of HepG2 cells.

For further elaboration of the SARs observed at EGFR-TK, molecular docking study of compound **21** into the active site of EGFR-TK was performed using

AutoDock 4.2.6 based on EGFR complex structure with Erlotinib (PDB code: 1M17). As depicted in **Fig. 4**, compound **21** is nicely bound to the ATP binding site of EGFR-TK. Compared to the binding model of Erlotinib, which N1of the quinazoline accepted an H-bond from Met769 and N3 formed an H-bond bridge formation through H_2O with Thr776; compound **21** occupied the same EGFR-TK binding pocked. Specially, there exists an H-bond with O atom at C-7 position interaction with Cys773, which might be favor to the EGFR-TK inhibitory activity. The model also showed that there is a π-π interaction and hydrophobic interaction between benzene ring in the side chain in the equatorial position and Phe771 and Tyr777, which maybe bring improved the EGFR-TK inhibitory activity.

Fig. 4

2.2.3 *In vitro* EGFR-TK inhibitory activity assay

Aiming to estimate the targeted effects of the designed compounds as TKIs, kinase inhibitory activity of compound **21** was evaluated through EGFR-TK activity assay by ELISA. Gefitinib, with high selectivity and potency to EGFR-TK, was chosen as a positive drug in our kinase assay. The experimental results were showed in **Table 7**. The inhibitory activities are given as OD values and percentage inhibition at various concentrations of the compound **21**. The concentration-dependent inhibitory curves were shown in **Fig. 5** and the IC_{50} values were listed in **Table 8**. Specifically speaking, compound **21** displayed potent inhibitory activity at nanomolar concentration level with a dose-dependent manner (IC_{50} = 3.62 nM for EGFR-TK), which is slightly weaker comparable to the positive control Gefitinib (IC_{50} = 2.21 nM for EGFR-TK). Differences between groups were considered statistically significant at $^{*}P < 0.05$. Therefore, we could conclude that compound **21** can inhibit the function of EGFR-TK and the anti-proliferative activity was produced partly by the interaction between EGFR-TK and the tested compound.

Table 7

Fig. 5

Table 8

2.2.4 LDH activities detecting the cytotoxicity of compound **21**

The cytotoxicity of compound **21** against HepG2 cells was tested by LDH release activities at 48 h, and Gefitinib was used as a positive control drug. The tested results are shown in **Table 9** and **Fig.6**. Comparing to full release group and natural release group, it is found that the cytotoxicity on HepG2 cells of compound **21** was very low at different concentrations, and the change of the value with the concentration is not obvious, which is similar to that of Gefitinib. It was confirmed that compound **21** was anti-proliferative rather than cytotoxicity on HepG2 cells and its mechanism of action may be similar to Gefitinib. Significant differences between groups were considered statistically significant at $^{*}P < 0.05$.

Table 9

Fig. 6

2.2.5 Cell cycle analysis on HepG2 cells by flow cytometry

In order to better elucidate that the mechanism of proliferation inhibition was associated with cell cycle arrest, cell cycle distribution on HepG2 cells by treating with various concentrations (0, 2.5, 5.0 and 10.0 μM) of compound **21** was performed. As depicted in **Table 10** and **Fig. 7-8**, the region marked with different colors represents % population at different phases of the cell cycle. Significant changes in cell cycle profile can be detected through a concentration-dependent manner increase of cells in S phase together with a concomitant decrease of G0/G1 phase cells after 48 h of incubation, which is consistent with the one of the most efficient antitumor drug Gefitinib, as a reference.

Table 10

Fig. 7 and Fig. 8

Concretely speaking, compound **21** caused an increase in the proportion of cells in S phase (from 21.46% in the control to 29.72% at 10.0 μM) in a concentration-dependent manner with a concomitant decrease of cells in G0/G1 phase of the cell cycle (from 69.40% in the control to 60.72% at 10.0 μM). These results confirmed that compound **21** arrested cell cycle progression dramatically on HepG2 cells, which eventually inhibited tumor cell proliferation in a dose-dependent manner by inducing S growth arrest and reducing the G0/G1 phase of the cell cycle and

resulted in cell apoptosis.

2.2.6 Induction of apoptosis assay on HepG2 cells

There are three types of programmed cell death in biological systems, namely autophagy, necrosis and apoptosis. Apoptosis is a series of biochemical events leading to morphological changes and cell death. It has been observed that many cytotoxic drugs show anticancer activities by inducing cell apoptosis. To further explain the inhibition of cell growth, we first evaluated compound **21**-induced apoptosis on HepG2 cells using AnnexinV-FITC and propidium iodide (PI) double staining by flow cytometry, which stain phosphatidylserine residues and DNA, respectively. The results were shown in **Table 11** and **Fig. 9-10**.

Table 11

Fig. 9 and Fig. 10

As can be seen, compound **21** is effective in induction of cell apoptosis in a dose-dependent manner. Treatment of HepG2 cells by 0, 2.5, 5.0 and 10.0 μM of compound **21** for 48 h results in 52.4%, 82.8% and 98.7% of apoptotic cells (early + late), as compared to 13.5% of apoptotic cells in an untreated control. This is consistent with its nice binding affinity to EGFR-TK and potent activity in inhibition of cell growth. These results revealed that compound **21** inhibited cell growth through cell apoptosis induction.

2.2.7 Morphology of cells by Fluorescence microscopy

Flow cytometry alone cannot conclusively identify apoptotic cells, the results were further corroborated by studying nuclear morphological changes of cells by fluorescence microscopy. To further confirm the induction of apoptosis, we monitored the morphological changes induced by compound **21** on HepG2 cells for Hoechst 33242 and PI double staining. After exposure to the various concentrations of compound **21** for 48 h, the HepG2 cells showed significant evidence of apoptosis mediated cell death, including chromatin condensation and nuclear fragmentation. Cell morphology was investigated using fluorescence microscopy. As reflected in **Fig. 11**, it can be observed that the control cells showed the homogeneous blue fluorescence in the nuclei without red-orange fluorescence as these cells cannot take up PI staining solution, which suggested that there was no obvious nuclear condensation and fragmentation in HepG2 cells. However, when the cells treated with compound **21**, the nuclei became convoluted and budded off into several fragments, and nuclear condensation and fragmentation were observed in the pictures, indicating a typical characteristic of apoptosis. Moreover, the treated cells exhibited red-orange fluorescence due to staining with PI because apoptotic cells with ruptured membrane allow the entry of PI to intercalate into DNA. Furthermore, it is found that more and

more cells stained in dark blue were observed under the microscope as the increase of concentration from 2.5 to 20 μM. It is suggested that compound **21** induce the cellular apoptosis dose-dependently, which is consistent with the former anti-proliferation activity assay.

Fig. 11

2.2.8 Effect on mitochondrial membrane potential loss

Impairment in mitochondrial function is an early event in the executive phase of programmed cell death in various cell types, and appears as the result of a preliminary decrease in the mitochondrial membrane potential(MMP), which is crucial for caspase-dependent and caspase-independent apoptotic cell death pathways. The effect of compound **21** on MMP loss in HepG2 cells was performed. The MMP loss in untreated and treated groups is measured by Rhodamine-123 dye (Rh-123) which is reduced by healthy mitochondria into fluorescent probe whose fluorescence is measured by flow cytometry. As depicted in **Table 12**, **Fig. 12-13**, compound **21** treated HepG2 cells for 48 h showed loss of MMP with 2.1%, 3.4%, 6.4% and 34.5% at 2.5, 5, 10 and 20 μM, respectively. The results indicated that the rationality and possibility of mitochondria-mediated cell death. Significant differences between groups were considered statistically significant at $^{*}P < 0.05$, $^{**}P < 0.01$.

Table 12

Fig. 12 and Fig. 13

2.2.9 Detection of the intracellular level of Ca^{2+} concentration

Ca^{2+} as a second messenger for cellular functions may play an important role in the regulation of apoptosis through mitochondria-mediated apoptosis pathway, which can activate caspase-3 that direct executors of apoptosis, and induce cell apoptosis. The intracellular free Ca^{2+} concentration was detected using the fluorescence Ca^{2+} indicator Fluo-3/AM, and the results were shown in **Table 13** and **Fig. 14**. Statistical analysis showed that the concentration of intracellular free Ca^{2+} in each drug treatment group increased obviously compared with the negative control group (from 41.7% to 52.7% *vs.* 14.2% of the negative control group), indicating that compound **21** can cause the rise of intracellular free Ca^{2+} concentration in the early phase of apoptosis with a concentration dependent manner, which can indicate the opening of mitochondrial permeability transition pore. These results suggested that Ca^{2+} may be involved in signal transduction in apoptotic cell death in HepG2 cells *via* Ca^{2+}-mediated mitochondrial damage. Significant differences between groups were

considered statistically significant at $^{*}P < 0.05$, $^{**}P < 0.01$, $^{***}P < 0.001$.

Table 13

Fig. 14

2.2.10 Detection of the intracellular level of ROS

Reactive oxygen species (ROS) may also function as secondary messengers in cell signaling transduction pathways and cell cycle events, which are associated with the apoptosis mediated by mitochondria, endoplasmic reticulum and death receptor. The production of ROS was detected by the DCFH-DA capture agent to capture ROS. The experimental results were presented in **Fig. 15**. The green fluorescence intensity of DCF that was produced by DCFH through the oxidization by ROS was proportional to the level of ROS. The results showed that the production of ROS levels were significantly increased in HepG2 cells treated with different concentrations of the target compound **21** for 48 h in comparison with the negative control group, and indicated that compound **21** treated with HepG2 cells can induce the elevation of ROS levels with a concentration-dependent manner, which may have an influence on the changes of MMP, and may be involved in ROS-mediated cell apoptosis through mitochondrial pathway.

Fig. 15

2.2.11 Detection of intracellular caspase-3 activity

Cysteinyl aspartate-specific proteases (caspase) show a crucial role in the process of cell apoptosis. Particularly, caspase-3 is called executer of cell apoptosis and an important part of the molecular mechanism of apoptosis, which is related to the fragmentation of DNA, the accumulation of chromatin condensation and formation of apoptosome. To further confirm the induction of apoptosis by compound **21**, the activation of caspase-3 in the apoptotic cells was carried out. In order to determine the degree of activation of caspase-3, we used the caspase-3 sequence-specific peptide substrate coupled to chromophore group, when the substrate was cut by caspase-3 in the cells, the chromophore was free, the absorbance was measured by a microplate reader, and the results were shown in **Table 14** and **Fig.16**. Statistical analysis results showed that caspase-3 activities were significantly enhanced by different concentrations of compound **21** in HepG2 cells for 48 h in a concentration dependent manner, compared with the negative control group. These results indicated caspase-3 is activated during apoptosis and compound **21** selectively inhibits proliferation of HepG2 cells via activating caspase-3-mediated apoptosis. Significant differences

between groups were considered statistically significant at $^{*}P< 0.05$, $^{**}P < 0.01$.

Table 14

Fig. 16

---

3. Conclusions

In this work, a series of novel 4-aminoquinazoline derivatives as potent EGFR-TKIs have been reported. The results showed that most compounds displayed certain inhibition activities against the selected human cancer cells, and some compounds exhibited better broad-spectrum inhibition activities than Gefitinb and QWL-22b. It can be observed that the presence of substituents and their properties strongly influenced the anti-proliferative activities. The IC_{50} values of compound **21** against HepG2, A549, MCF-7, DU145 and SH-SY5Y cells were much lower than those of Gefitinb, however, the IC_{50} value of compound **21** against CCC-HPF-1 cells was similar to that of Gefitinib. Compound **21** demonstrated more potent EGFR-TK inhibitory activity with the IC_{50} of 3.62 nM, similar to that of Gefitinib (2.21 nM). LDH release assay proved that compound **21** was anti-proliferative rather than cytotoxicity in HepG2 cells. Compound **21** caused S phase arrest and induced cell apoptosis to inhibit cell proliferation. Effects of MMP in HepG2 cells, and the determination of intracellular free Ca^{2+} concentration, ROS and caspase-3 activity indicated that compound **21** could induce apoptosis through mitochondria-mediated apoptotic pathway and caspase-3-mediated mechanism. In general, compound **21** exerts potential antitumor activity through several mechanisms, including anti-proliferation, cell cycle arrest and pro-apoptotic effects *via* the mitochondrial-mediated caspase-dependent pathway, and may serve as model molecule to help us to further design and develop more potent anticancer agents, and also further investigate their mechanisms of action.

4. Experimental sections

4.1. Synthesis and characterization of target compounds

4.1.1. General methods/instruments

All commercially available starting materials, reagents and solvents were used without further purification. All the reactions were routinely monitored by thin-layer chromatography (TLC) in silica gel (GF254 Merck plates) and the products visualized with ultraviolet lamp (254 nm and 365 nm). Column chromatography separations were obtained on silica gel (200-300 mesh). Melting points were recorded on a RY-1 melting point apparatus and are uncorrected. ^{1}H NMR and ^{13}C NMR spectra were determined in DMSO-d_6 solutions using a Bruker Avance 400 MHz spectrometer with TMS as the internal standard, and the values of the chemical shifts (δ) were given in

ppm, coupling constants values (*J*) are given in Hz. Mass spectra (MS) were performed on a LCT Premier XE (ESI) or 320-MS (EI) mass spectrometry. Chemical names were created using ChemBioDraw Ultra 12.0 software.

4.1.2. Synthetic procedures

4.1.2.1. Synthesis of methyl 4-(3-chloropropoxy)-3-methoxybenzoate (**2**)

To a stirred solution of methyl vanillate **1** (10.0 g, 0.055 mol) in DMF (300 mL) were added K_2CO_3 (10.4 g, 0.066 mol) and 1-bromo-3-chloropropane (11.4 g, 0.082 mol). The mixture was heated at 60□ for 5 h. After the reaction mixture was cooled to room temperature and poured into ice water (400 mL). After being stirred for 1 h, the respective product was filtered off, washed with ice water and dried to obtain the crude intermediate **2** as a white solid, which was used without purification. Yield: 97%, m.p.: 98-100□.

4.1.2.2. Synthesis of methyl 4-(3-chloropropoxy)-5-methoxy-2-nitrobenzoate (**3**)

To a stirred solution of crude **2** (10.0 g, 0.039 mol) in AcOH (35 mL) was slowly added 65% HNO_3 (8 mL) at 0-5□.Subsequently, the mixture was heated to 50□ for 5 h, then cooled to room temperature and poured into ice water(300 mL). After being stirred for 1 h, the product was extracted with ethyl acetate (3×25 mL), the combined organic layer was washed with water, saturated sodium bicarbonate and saturated sodium chloride, and then dried with anhydrous Na_2SO_4. The ethyl acetate was removed under reduced pressure to afford the nitration product **3** as yellow oil. Yield: 88%, m.p.: 64-66□.

4.1.2.3. Synthesis of methyl 2-amino-4-(3-chloropropoxy)-5-methoxybenzoate (**4**)

A solution of **3** (6.0 g, 0.02 mol) in AcOH (35 mL) was stirred for 30 min at 80□, and powdered iron (3.5 g, 0.06 mol) was added. The mixture was stirred for another 40 min at 80□, and then the mixture was slowly poured into ice water and extracted with ethyl acetate (3×30 mL). The organic layer was washed with water, saturated sodium bicarbonate and saturated sodium chloride, and then dried with anhydrous Na_2SO_4. The solvent was evaporated under reduced pressure to yield reduction product **4**. The brown solid residue was recrystallized from ethyl acetate/petroleum ether to give a white solid. Yield: 82%, m.p.: 97-99□.

4.1.2.4. Synthesis of 7-(3-chloropropoxy)-6-methoxyquinazolin-4(3H)-one (**5**)

A mixture of formamidine acetate (5.0 g, 38 mmol), and crude **4** (5.0 g, 18 mmol) in EtOH (40 mL) was heated at reflux for 6 h. The mixture was cooled to room temperature, and then the precipitate was collected by filtration, washed with cold ethanol and dried to get **5** as a white powder. Yield: 90%, m.p.:218-220□.

4.1.2.5. Synthesis of 4-chloro-7-(3-chloropropoxy)-6-methoxyquinazoline (**6**)

The mixture of **5** (2.0 g, 7.5 mmol) and $POCl_3$ (10 mL) was stirred at reflux for 4 h. The solution was concentrated under reduced pressure to dryness and excess ethyl acetate was added. The solution was washed with water and brine, dried with anhydrous Na_2SO_4 and concentrated to afford the pure compound **6** as a yellow solid. Yield: 95%, m.p.:126-128□.

4.1.2.6. General process for the synthesis of **7a-c**

To a stirred solution of **6** (1.0 g, 3.5 mmol) in isopropanol (20 mL) was added aminobenzonitrile (0.5 g, 4.3 mmol). The mixture was heated under reflux for 2 h and

cooled to room temperature. The light-yellow solid was filtered, washed and dried to yield compounds **7a-c**.

4.1.2.6.1. 4-((7-(3-chloropropoxy)-6-methoxyquinazolin-4-yl)amino)benzonitrile (**7a**). Yield: 95%, m.p.:126-128□. ^{1}H NMR (400 MHz, DMSO-d_6): δ 9.78 (s, 1H, NH), 8.58 (s, 1H, ArH), 8.13 (s, 1H, ArH), 8.11 (s, 1H, ArH), 7.85-7.82(m, 3H, ArH), 7.27 (s, 1H, ArH), 4.28 (t, *J* = 8.0 Hz, 2H, -O***CH₂***CH_2CH_2Cl), 3.99 (s, 3H, -OCH_3), 3.82 (t, *J* = 8.0 Hz, 2H, -OCH_2CH_2***CH₂***Cl), 2.30-2.24 (m, 2H, -OCH_2***CH₂***CH_2Cl). ESI-MS: m/z calcd found 370.13 [M+H] $^+$. Anal. calcd: C 61.84, H 4.63, Cl 9.63, N 15.21, O 8.69.

4.1.2.6.2. 3-((7-(3-chloropropoxy)-6-methoxyquinazolin-4-yl)amino)benzonitrile (**7b**). Yield: 93%, m.p.:126-128□. ^{1}H NMR (400 MHz, DMSO-d_6): δ 9.68 (s, 1H, NH), 8.55 (s, 1H, ArH), 8.37 (s, 1H, ArH), 8.13 (d, *J* = 8.1 Hz, 1H, ArH), 7.84 (s, 1H, ArH), 7.55(dd, *J* = 21.1, 7.8 Hz, 2H, ArH), 7.24 (s, 1H, ArH), 4.27 (s, 2H, -O***CH₂***CH_2CH_2Cl), 3.98 (s, 3H, -OCH_3), 3.82 (s, 2H, -OCH_2CH_2***CH₂***Cl), 2.26 (m, 2H, -OCH_2***CH₂***CH_2Cl). ESI-MS: m/z calcd found 370.15 [M+H] $^+$. Anal. calcd: C 61.83, H 4.65, Cl 9.61, N 15.22, O 8.69.

4.1.2.6.3. 2-((7-(3-chloropropoxy)-6-methoxyquinazolin-4-yl)amino)benzonitrile (**7c**). Yield: 90%, m.p.:126-128□. ^{1}H NMR (400 MHz, DMSO-d_6): δ 9.65 (s, 1H, NH), 8.48 (s, 1H, ArH), 8.13 (d, *J* = 8.7 Hz, 1H, ArH), 8.06 (d, *J* = 8.04 Hz, 1H, ArH), 7.62-7.58 (m, 2H, ArH), 7.26 (s, 1H, ArH), 7.20 (s, 1H, ArH), 4.17 (s, 2H, -O***CH₂***CH_2CH_2Cl), 3.92 (s, 3H, -OCH_3), 3.62 (s, 2H, -OCH_2CH_2***CH₂***Cl), 2.12 (m, 2H, -OCH_2***CH₂***CH_2Cl). ESI-MS: m/z calcd found 370.13 [M+H] $^+$. Anal. calcd: C 61.89, H 4.64, Cl 9.62, N 15.22, O 8.62.

4.1.2.7. General process for the synthesis of the title compounds (**8-41**)

To a stirred solution of compounds **7a-c** (0.25 g, 0.68 mmol) in DMF (5 mL) was added K_2CO_3 (1.5:1), KI (0.01:1) and various substituted aniline (1.5:1). The solution was heated at 80□ for 6-10 h. Then the reaction mixture was cooled to room temperature, diluted with water (200 mL) and extracted with ethyl acetate (3×20 mL), combined organic layer, washed with brine, dried with anhydrous Na_2SO_4 and concentrated under vacuum to afford the target products as a solid. Compounds **8-41** were characterized as follows.

4.1.2.7.1.

4-((7-(3-(dimethylamino)propoxy)-6-methoxyquinazolin-4-yl)amino)benzonitrile (**8**) Yield: 88%, m.p.:170-172□. ^{1}H NMR (400 MHz, DMSO-d_6): δ 9.78 (s, 1H, NH), 8.58 (s, 1H, ArH), 8.12 (d, *J* = 8.5 Hz, 2H, ArH), 8.04 (m, 3H, ArH), 7.27 (s, 1H, ArH), 4.28 (m, 2H, -O***CH₂***CH_2CH_2N-), 3.99 (s, 3H, -OCH_3), 2.69 (m, 2H, -N***CH₂***CH_2CH_2O-), 2.18 (s, 6H, -CH_3), 1.85 (m, 2H, -OCH_2***CH₂***CH_2N-). ^{13}C NMR (100 MHz, DMSO-d_6): δ 158.61, 156.59, 156.01, 149.85, 148.49, 144.85, 131.05, 126.71, 113.06, 108.81, 106.09, 102.76, 69.87, 56.06, 54.66, 49.24, 26.78. ESI-MS: m/z calcd found 378.13 [M+H] $^+$. Anal. calcd: C 66.85, H 6.16, N 18.53, O 8.46.

4.1.2.7.2.

4-((7-(3-(diethylamino)propoxy)-6-methoxyquinazolin-4-yl)amino)benzonitrile (**9**) Yield: 90%, m.p.:178-181□. ^{1}H NMR (400 MHz, DMSO-d_6): δ 9.78 (s, 1H, NH), 8.58 (s, 1H, ArH), 8.12 (d, *J* = 8.5 Hz, 2H, ArH), 8.03 (m, 3H, ArH), 7.23 (s, 1H,

ArH), 4.28 (m, 2H, -O***CH₂***CH_2CH_2N-), 3.99 (s, 3H, -OCH_3), 2.89 (m, 4H, -N***CH₂***CH_3), 2.59 (m, 2H, -N***CH₂***CH_2CH_2O-), 1.87 (m, 2H, -OCH_2***CH₂***CH_2N-), 1.01 (t, 6H, -NCH_2***CH₃***). ^{13}C NMR (100 MHz, DMSO-d_6): δ 158.82, 156.67, 156.53, 149.99, 148.87, 145.05, 131.65, 126.91, 113.24, 108.99, 106.19, 102.89, 71.09, 57.13, 54.86, 52.97, 26.78, 15.46. ESI-MS: m/z calcd found 406.33 $[M+H]^+$. Anal. calcd: C 68.14, H 6.76, N 12.26, O 7.84.

4.1.2.7.3.

4-((7-(3-((2-hydroxyethyl)(methyl)amino)propoxy)-6-methoxyquinazolin-4-yl)amino) benzonitrile (**10**) Yield: 83%, m.p.:218-220□. ^{1}H NMR (400 MHz, DMSO-d_6): δ 9.78 (s, 1H, NH), 8.58 (s, 1H, ArH), 8.11 (d, *J* = 8.5 Hz, 2H, ArH), 8.03 (m, 3H, ArH), 7.23 (s, 1H, ArH), 4.18 (m, 2H, -O***CH₂***CH_2CH_2N-), 3.99 (s, 3H, -OCH_3), 3.46 (t, 2H, -***CH₂***OH), 2.45-2.61 (m, 4H, -N*CH₂*-), 2.21(s, 3H, -NCH_3), 1.89 (m, 2H, -OCH_2***CH₂***CH_2N-). ^{13}C NMR (100 MHz, DMSO-d_6): δ 158.57, 156.48, 155.76, 149.54, 148.23, 144.35, 130.77, 126.15, 113.01, 108.62, 106.03, 102.21, 69.56, 58.89, 55.84, 54.04, 53.03, 48.77, 26.65. ESI-MS: m/z calcd found 408.23 $[M+H]^+$. Anal. calcd: C 64.87, H 6.17, N 17.20, O11.76.

4.1.2.7.4.

4-((7-(3-(bis(2-hydroxyethyl)amino)propoxy)-6-methoxyquinazolin-4-yl)amino)benz onitrile (**11**) Yield: 73%, m.p.:162-164□. ^{1}H NMR (400 MHz, DMSO-d_6): δ 9.78 (s, 1H, NH), 8.58 (s, 1H, ArH), 8.11 (d, *J* = 8.5 Hz, 2H, ArH), 8.03 (m, 3H, ArH), 7.23 (s, 1H, ArH), 4.18 (m, 2H, -O***CH₂***CH_2CH_2N-), 3.99 (s, 3H, -OCH_3), 3.46-3.52 (m, 4H, -CH_2***CH₂***OH), 2.45-2.63 (m, 6H, -N*CH₂*-), 1.87 (m, 2H, -OCH_2***CH₂***CH_2N-). ^{13}C NMR (100 MHz, DMSO-d_6): δ 158.68, 156.56, 155.79, 149.68, 148.57, 144.51, 130.82, 126.35, 113.23, 108.77, 106.34, 102.45, 70.53, 58.09, 55.25, 54.87, 54.34, 26.89. ESI-MS: m/z calcd found 438.20 $[M+H]^+$. Anal. calcd: C 63.13, H 6.25, N 16.02, O 14.60.

4.1.2.7.5.

4-((7-(3-(benzyl(methyl)amino)propoxy)-6-methoxyquinazolin-4-yl)amino)benzonitri le (**12**) Yield: 84%, m.p.:234-236□. ^{1}H NMR (400 MHz, DMSO-d_6): δ 9.71 (s, 1H, NH), 8.48 (s, 1H, ArH), 8.03 (q, 2H, ArH), 7.79 (s, 1H, ArH), 7.73 (q, 2H, ArH), 7.42 (t, 2H, ArH), 7.34 (m, 2H, ArH), 7.26 (m, 2H, ArH), 5.21 (s, 2H, Ar*CH₂*-), 4.18 (m, 2H, -O***CH₂***CH_2CH_2N-), 3.89 (s, 3H, -OCH_3), 2.63 (m, 2H, -N*CH₂*-), 2.56 (s, 3H, -NCH_3), 1.87 (m, 2H, -OCH_2***CH₂***CH_2N-). ^{13}C NMR (100 MHz, DMSO-d_6): δ 158.76, 156.66, 156.01, 152.85, 148.49, 145.85, 139.18, 131.15, 128.71, 127.83, 127.56, 119.78, 113.86, 108.89, 106.27, 102.88, 69.87, 62.89, 55.03, 53.36, 42.34, 25.97. ESI-MS: m/z calcd found 454.22 $[M+H]^+$. Anal. calcd: C 71.52, H 6.01, N 15.42, O 7.05.

4.1.2.7.6.

4-((7-(3-(benzyl(2-hydroxyethyl)amino)propoxy)-6-methoxyquinazolin-4-yl)amino)b enzonitrile (**13**) Yield: 87%, m.p.:215-218□. ^{1}H NMR (400 MHz, DMSO-d_6): δ 9.83 (s, 1H, NH), 8.48 (s, 1H, ArH), 8.03 (d, 2H, ArH), 7.83 (s, 1H, ArH), 7.73 (d, 2H, ArH), 7.41 (t, 2H, ArH), 7.34 (m, 2H, ArH), 7.26 (m, 2H, ArH), 5.19 (s, 2H, Ar*CH₂*-), 4.18 (m, 2H, -O***CH₂***CH_2CH_2N-), 3.89 (s, 3H, -OCH_3), 2.45-2.63 (m, 4H, -N*CH₂*-), 3.46-3.52 (m, 2H, -CH_2***CH₂***OH), 1.89 (m, 2H, -OCH_2***CH₂***CH_2N-). ^{13}C NMR (100

MHz, DMSO-d_6): δ 158.89, 156.76, 156.23, 152.88, 148.53, 145.88, 139.24, 131.27, 128.88, 127.87, 127.65, 119.74, 113.88, 108.94, 106.33, 102.92, 70.37, 63.89, 56.06, 55.66, 54.74, 52.82, 26.69. ESI-MS: m/z calcd found 484.21 $[M+H]^+$. Anal. calcd: C 69.57, H 6.02, N 14.46, O 9.95.

4.1.2.7.7.

4-((6-methoxy-7-(3-(pyrrolidin-1-yl)propoxy)quinazolin-4-yl)amino)benzonitrile (**14**) Yield: 83%, m.p.:160-162□. ^{1}H NMR (400 MHz, DMSO-d_6): δ 9.78 (s, 1H, NH), 8.58 (s, 1H, ArH), 8.12 (d, *J* = 8.5 Hz, 2H, ArH), 8.04 (m, 3H, ArH), 7.23 (s, 1H, ArH), 4.20 (m, 2H, -O***CH₂***CH_2CH_2N-), 3.99 (s, 3H, -OCH_3), 2.58 (m, 2H, -NCH_2-), 2.50 (m, 2H, -NCH_2-), 2.10-1.93 (m, 2H, -N***CH₂***CH_2CH_2O-), 1.91 (m, 2H, -OCH_2***CH₂***CH_2N-), 1.70 (m, 4H, -CH_2CH_2-). ^{13}C NMR (100 MHz, DMSO-d_6): δ 158.77, 156.68, 156.21, 149.89, 148.57, 144.89, 131.32, 126.86, 113.23, 108.88, 106.21, 102.87, 69.99, 56.28, 54.66, 53.87, 25.99, 22.78. ESI-MS: m/z calcd found 404.33 $[M+H]^+$. Anal. calcd: C 68.49, H 6.23, N 13.38, O 7.91.

4.1.2.7.8.

4-((6-methoxy-7-(3-(piperidin-1-yl)propoxy)quinazolin-4-yl)amino)benzonitrile (**15**) Yield: 81%, m.p.:172-174□. ^{1}H NMR (400 MHz, DMSO-d_6): δ 9.78 (s, 1H, NH), 8.58 (s, 1H, ArH), 8.12 (d, *J* = 8.5 Hz, 2H, ArH), 7.92-7.78 (m, 3H, ArH), 7.23 (s, 1H, ArH), 4.19 (t, 2H, -O***CH₂***CH_2CH_2N-), 3.99 (s, 3H, -OCH_3), 1.95 (dd, *J* = 17.5, 10.8 Hz, 6H, -NCH_2-), 1.60-1.38 (m, 8H, -OCH_2***CH₂***CH_2N- and -$CH_2CH_2CH_2$-). ^{13}C NMR (100 MHz, DMSO-d_6): δ 158.75, 156.67, 156.31, 149.91, 148.53, 144.89, 131.17, 126.89, 113.33, 108.92, 106.22, 102.88, 69.76, 56.21, 55.34, 54.72, 26.89, 24.33, 23.28. ESI-MS: m/z calcd found 418.33 $[M+H]^+$. Anal. calcd: C 69.06, H 6.51, N 16.75, O 7.68.

4.1.2.7.9.

4-((6-methoxy-7-(3-(4-methylpiperidin-1-yl)propoxy)quinazolin-4-yl)amino)benzonitrile (**16**) Yield: 85%, m.p.:170-172□. ^{1}H NMR (400 MHz, DMSO-d_6): δ 9.78 (s, 1H, NH), 8.58 (s, 1H, ArH), 8.13 (d, *J* = 8.6 Hz, 2H, ArH), 7.97-7.77 (m, 3H, ArH), 7.23 (s, 1H, ArH), 4.18 (t, 2H, -O***CH₂***CH_2CH_2N-), 3.99 (s, 3H, -OCH_3), 2.88 (t, *J* = 10.6 Hz, 2H, -N***CH₂***CH_2CH_2O-), 1.58 (t, *J* = 12.6 Hz, 4H, -NCH_2-), 1.38-1.13 (m, 10H, -OCH_2***CH₂***CH_2N- and piperidine-H, -CH_3). ^{13}C NMR (100 MHz, DMSO-d_6): δ 158.77, 156.58, 156.33, 149.93, 148.52, 144.85, 131.27, 126.93, 113.45, 108.87, 106.32, 102.84, 69.88, 56.06, 54.34, 45.89, 31.33, 30.87, 26.65, 19.28. ESI-MS: m/z calcd found 432.42 $[M+H]^+$. Anal. calcd: C 69.56, H 6.79, N 16.20, O 7.45.

4.1.2.7.10.

4-((7-(3-(4-hydroxypiperidin-1-yl)propoxy)-6-methoxyquinazolin-4-yl)amino)benzonitrile (**17**) Yield: 82%, m.p.:194-196□. ^{1}H NMR (400 MHz, DMSO-d_6): δ 9.78 (s, 1H, NH), 8.58 (s, 1H, ArH), 8.11 (d, *J* = 8.6 Hz, 2H, ArH), 7.97 (m, 3H, ArH), 7.23 (s, 1H, ArH), 4.18 (t, 2H, -O***CH₂***CH_2CH_2N-), 3.99 (s, 3H, -OCH_3), 3.67 (m, 1H, -***CH***OH), 2.82-2.77 (m, 4H, -NCH_2-), 2.31-2.55 (m, 2H, -NCH_2-), 1.91-1.61 (m, 6H, -OCH_2***CH₂***CH_2N- and -NCH_2***CH₂***-). ^{13}C NMR (100 MHz, DMSO-d_6): δ 158.86, 156.65, 156.43, 149.89, 148.68, 144.89, 131.43, 126.99, 113.61, 108.92, 106.45, 102.88, 70.87, 62.84, 55.86, 54.34, 42.78, 30.38, 25.88. ESI-MS: m/z calcd found 434.32 $[M+H]^+$. Anal. calcd: C 66.48, H 6.29, N 16.14, O 11.09.

4.1.2.7.11.

4-((7-(3-(4-(hydroxymethyl)piperidin-1-yl)propoxy)-6-methoxyquinazolin-4-yl)amino)benzonitrile (**18**) Yield: 87%, m.p.:262-264□. ^{1}H NMR (400 MHz, DMSO-d_6): δ 9.78 (s, 1H, NH), 8.58 (s, 1H, ArH), 8.11 (d, J = 8.6 Hz, 2H, ArH), 7.97 (m, 3H, ArH), 7.23 (s, 1H, ArH), 4.18 (t, 2H, -O***CH₂***CH_2CH_2N-), 3.99 (s, 3H, -OCH_3), 3.63 (s, 2H, -***CH₂***OH), 2.89-2.77 (m, 6H, -NCH_2-), 2.14 (m, 2H, -OCH_2***CH₂***CH_2N-), 1.73-1.31 (m, 5H, -***CH***CH_2OH and -NCH_2***CH₂***-). ^{13}C NMR (100 MHz, DMSO-d_6): δ 158.77, 156.67, 156.52, 149.81, 148.72, 144.85, 131.55, 126.83, 113.76, 108.89, 106.56, 102.82, 70.45, 62.02, 55.77, 54.65, 45.76, 32.38, 25.88, 24.02. ESI-MS: m/z calcd found 448.32 [M+H] $^{+}$. Anal. calcd: C 67.06, H 6.56, N 15.62, O 10.77.

4.1.2.7.12.

4-((7-(3-(2-(2-hydroxyethyl)piperidin-1-yl)propoxy)-6-methoxyquinazolin-4-yl)amino)benzonitrile (**19**) Yield: 84%, m.p.:194-196□. ^{1}H NMR (400 MHz, DMSO-d_6): δ 9.78 (s, 1H, NH), 8.58 (s, 1H, ArH), 8.11 (d, J = 8.5 Hz, 2H, ArH), 7.96-7.78 (m, 3H, ArH), 7.23 (s, 1H, ArH), 4.17 (t, 2H, -O***CH₂***CH_2CH_2N-), 3.99 (s, 3H, -OCH_3), 3.87 (t, 2H, -CH_2***CH₂***OH), 2.87-2.57 (m, 5H, -NCH_2-), 1.99 (m, 2H, -OCH_2***CH₂***CH_2N-), 1.65-1.37 (m, 8H, -***CH₂***CH_2OH and -$CH_2CH_2CH_2$-). ^{13}C NMR (100 MHz, DMSO-d_6): δ 158.89, 156.76, 156.65, 149.89, 148.84, 144.89, 131.64, 126.91, 113.88, 108.92, 106.66, 102.89, 70.89, 63.52, 60.17, 55.24, 54.58, 49.76, 32.88, 30.23, 25.88, 23.82, 21.03. ESI-MS: m/z calcd found 462.34 [M+H] $^{+}$. Anal. calcd: C 67.64, H 6.76, N 15.19, O 10.41.

4.1.2.7.13. Ethyl 1-(3-((4-((4-cyanophenyl)amino)-6-methoxyquinazolin-7-yl)oxy)propyl)piperidine-4-carboxylate (**20**) Yield: 80%, m.p.:192-194□. ^{1}H NMR (400 MHz, DMSO-d_6): δ 9.78 (s, 1H, NH), 8.58 (s, 1H, ArH), 8.13 (d, J = 8.6 Hz, 2H, ArH), 7.97-7.77 (m, 3H, ArH), 7.23 (s, 1H, ArH), 4.18 (t, 2H, -O***CH₂***CH_2CH_2N-), 3.99 (s, 3H, -OCH_3), 2.87 (m, 6H, -N***CH₂***CH_2-), 2.28 (m, 1H, -*CH*CO-), 2.21-2.12 (m, 8H, -NCH_2***CH₂***-, -OCH_2***CH₂***CH_2N- and -O***CH₂***CH_3), 1.38 (t, 3H, -OCH_2***CH₃***). ^{13}C NMR (100 MHz, DMSO-d_6): δ 168.35, 158.27, 156.62, 156.23, 149.88, 148.54, 144.77, 131.16, 126.78, 113.33, 108.89, 106.21, 102.85, 69.98, 59.06, 55.21, 54.68, 52.24, 39.67, 27.06, 25.78, 12.89. ESI-MS: m/z calcd found 490.24 [M+H] $^{+}$. Anal. calcd: C 66.23, H 6.37, N 14.29, O 13.11.

4.1.2.7.14.

4-((6-methoxy-7-(3-(4-phenylpiperidin-1-yl)propoxy)quinazolin-4-yl)amino)benzonitrile (**21**) Yield: 82%, m.p.:194-196□. ^{1}H NMR (400 MHz, DMSO-d_6): δ 9.69 (s, 1H, NH), 8.47 (d, 1H, ArH), 8.03 (d, J = 8.7 Hz, 2H, ArH), 7.85-7.71 (m, 4H, ArH), 7.56 (m, 3H, ArH), 7.24-7,03 (m, 2H, ArH), 4.13 (t, 2H, -O***CH₂***CH_2CH_2N-), 3.89 (s, 3H, -OCH_3), 2.85 (m, 1H, -*CH*Ar), 2.12 (m, 2H, -OCH_2***CH₂***CH_2N-), 1.88-1.855 (m, 6H, -NCH_2-), 1.68–1.41 (m, 4H, -NCH_2***CH₂***-). ^{13}C NMR (100 MHz, DMSO-d_6): δ 158.76, 156.63, 156.11, 149.88, 148.57, 147.68, 144.85, 131.15, 128.71, 127.91, 126.89, 126.07, 113.36, 108.89, 106.14, 102.76, 69.97, 55.06, 53.66, 45.24, 39.03, 30.23, 26.58. ESI-MS: m/z calcd found 494.25 [M+H] $^{+}$. Anal. calcd: C 73.03, H 6.35, N 14.18, O 6.44.

4.1.2.7.15.

4-((7-(3-(3,4-dihydroisoquinolin-2(1H)-yl)propoxy)-6-methoxyquinazolin-4-yl)amino)benzonitrile (**22**) Yield: 81%, m.p.:234-236□. ^{1}H NMR (400 MHz, DMSO-d_6): δ 9.78 (s, 1H, NH), 8.58 (s, 1H, ArH), 8.11 (d, *J* = 8.6 Hz, 2H, ArH), 7.97-7.68 (m, 3H, ArH), 7.23 (s, 1H, ArH), 7.03-7.12 (m, 4 H, ArH), 4.22 (t, 2H, -O***CH₂***CH_2CH_2N-), 3.99 (s, 3H, -OCH_3), 3.60 (s, 2H, -NCH_2-), 3.17 (d, 2H, -NCH_2***CH₂***-), 2.85-2.70 (m, 4H, -NCH_2-), 2.12-2.03 (m, 2H, -OCH_2***CH₂***CH_2N-). ^{13}C NMR (100 MHz, DMSO-d_6): δ 158.69, 156.67, 156.12, 149.89, 148.59, 144.97, 138.16, 137.65, 131.05, 128.47, 128.13, 127.87, 125.32, 113.23, 108.89, 106.21, 102.88, 70.87, 56.06, 53.56, 53.27, 50.87, 25.84, 25.08. ESI-MS: m/z calcd found 466.25 [M+H] $^{+}$. Anal. calcd: C 72.23, H 5.84, N 15.05, O 6.88.

4.1.2.7.16.

4-((7-(3-(4-(dimethylamino)piperidin-1-yl)propoxy)-6-methoxyquinazolin-4-yl)amino)benzonitrile (**23**) Yield: 79%, m.p.:180-182□. ^{1}H NMR (400 MHz, DMSO-d_6): δ 9.78 (s, 1H, NH), 8.58 (s, 1H, ArH), 8.11 (d, *J* = 8.6 Hz, 2H, ArH), 7.97 (m, 3H, ArH), 7.23 (s, 1H, ArH), 4.19 (t, 2H, -O***CH₂***CH_2CH_2N-), 3.97 (s, 3H, -OCH_3), 2.82-2.77 (m, 4H, -N*CH₂*-), 2.27 (s, 6H, -N*CH₃*), 2.21-2.05 (m, 3H, -N*CH₂*- and -CH-), 1.81 (m, 4H, -OCH_2***CH₂***CH_2N- and -N***CH₂***CH_2-), 1.51 (m, 2H, -N***CH₂***CH_2-). ^{13}C NMR (100 MHz, DMSO-d_6): δ 158.67, 156.64, 156.33, 149.88, 148.53, 144.91, 131.21, 126.81, 113.23, 108.91, 106.23, 102.88, 70.87, 68.89, 56.35, 53.86, 50.24, 40.89, 25.78, 25.67. ESI-MS: m/z calcd found 461.42 [M+H] $^{+}$. Anal. calcd: C 67.82, H 7.03, N 18.22, O 6.93.

4.1.2.7.17.

4-((7-(3-([1,4'-bipiperidin]-1'-yl)propoxy)-6-methoxyquinazolin-4-yl)amino)benzonitrile (**24**) Yield: 85%, m.p.:176-178□. ^{1}H NMR (400 MHz, DMSO-d_6): δ 9.78 (s, 1H, NH), 8.58 (s, 1H, ArH), 8.13 (d, *J* = 8.6 Hz, 2H, ArH), 7.91 (m, 3H, ArH), 7.23 (s, 1H, ArH), 4.21 (t, 2H, -O***CH₂***CH_2CH_2N-), 3.99 (s, 3H, -OCH_3), 2.82-2.47 (m, 10H, -N*CH₂*-), 2.17-2.05 (m, 3H, -OCH_2***CH₂***CH_2N- and -CH-), 1.81 (m, 2H, -NCH_2***CH₂***-), 1.61-1.51 (m, 8H, -$CH_2CH_2CH_2$- and -NCH_2***CH₂***-). ^{13}C NMR (100 MHz, DMSO-d_6): δ 158.89, 156.67, 156.57, 149.93, 148.63, 144.89, 131.63, 126.88, 113.16, 108.87, 106.23, 102.88, 71.02, 68.85, 56.01, 55.88, 53.66, 50.67, 27.59, 25.79, 24.74, 24.03. ESI-MS: m/z calcd found 501.32 [M+H] $^{+}$. Anal. calcd: C 69.58, H 7.26, N 16.79, O 6.37.

4.1.2.7.18.

4-((6-methoxy-7-(3-(4-methylpiperazin-1-yl)propoxy)quinazolin-4-yl)amino)benzonitrile (**25**) Yield: 83%, m.p.:162-164□. ^{1}H NMR (400 MHz, DMSO-d_6): δ 9.78 (s, 1H, NH), 8.58 (s, 1H, ArH), 8.12 (d, *J* = 8.5 Hz, 2H, ArH), 7.84 (m, 3H, ArH), 7.23 (s, 1H, ArH), 4.18 (t, 2H, -O***CH₂***CH_2CH_2N-), 3.99 (s, 3H, -OCH_3), 2.55-2.45 (m, 6H, -N*CH₂*-), 2.17 (s, 3H, -N*CH₃*), 2.02-1.80 (m, 6H, -N*CH₂*- and -OCH_2***CH₂***CH_2N-). ^{13}C NMR (100 MHz, DMSO-d_6): δ 158.89, 156.79, 156.33, 149.90, 148.65, 144.89, 131.31, 126.79, 113.76, 108.99, 106.32, 102.88, 70.87, 55.86, 54.57, 54.01, 52.23, 43.52, 25.88. ESI-MS: m/z calcd found 433.23 [M+H] $^{+}$. Anal. calcd: C 66.63, H 6.53, N 19.42, O 7.42.

4.1.2.7.19.

4-((7-(3-(4-ethylpiperazin-1-yl)propoxy)-6-methoxyquinazolin-4-yl)amino)benzonitri

le (**26**) Yield: 81%, m.p.:164-166□. ^{1}H NMR (400 MHz, DMSO-d_6): δ 9.78 (s, 1H, NH), 8.58 (s, 1H, ArH), 8.13 (d, *J* = 8.7 Hz, 2H, ArH), 7.89-7.81 (m, 3H, ArH), 7.23 (s, 1H, ArH), 4.19 (t, 2H, -O*CH*$_2$CH$_2$CH$_2$N-), 3.99 (s, 3H, -OCH$_3$), 1.95(m, 6H, -N*CH*$_2$-, -N***CH*$_2$**CH$_3$, -OCH$_2$***CH*$_2$**CH$_2$N-), 1.41-1.07 (m, 6H, -N*CH*$_2$-), 1.05 (m, 5H, -N*CH*$_2$- and -NCH$_2$***CH*$_3$**). ^{13}C NMR (100 MHz, DMSO-d_6): δ 158.89, 156.79, 156.35, 149.91, 148.67, 144.89, 131.34, 126.81, 113.76, 108.97, 106.32, 102.86, 70.89, 55.86, 54.59, 54.27, 53.25, 47.78, 25.98, 12.89. ESI-MS: m/z calcd found 447.25 [M+H] $^{+}$. Anal. calcd: C 67.23, H 6.73, N 18.85, O 7.19.

4.1.2.7.20.

4-((7-(3-(4-(2-hydroxyethyl)piperazin-1-yl)propoxy)-6-methoxyquinazolin-4-yl)amino)benzonitrile (**27**) Yield: 80%, m.p.:168-171□. ^{1}H NMR (400 MHz, DMSO-d_6): δ 9.78 (s, 1H, NH), 8.58 (s, 1H, ArH), 8.11 (d, *J* = 8.7 Hz, 2H, ArH), 7.81 (m, 3H, ArH), 7.23 (s, 1H, ArH), 4.09 (t, 2H, -O***CH*$_2$**CH$_2$CH$_2$N-), 3.99 (s, 3H, -OCH$_3$), 3.49 (t, 2H, -NCH2***CH*$_2$**OH), 3.25-2.89 (m, 12H, -N*CH*$_2$-), 1.95 (m, 2H, -OCH$_2$***CH*$_2$**CH$_2$N-). ^{13}C NMR (100 MHz, DMSO-d_6): δ 158.88, 156.76, 156.43, 149.88, 148.56, 144.95, 131.43, 126.79, 113.37, 108.96, 106.17, 102.87, 71.04, 57.87, 57.78, 56.16, 55.96, 53.24, 26.38. ESI-MS: m/z calcd found 463.25 [M+H] $^{+}$. Anal. calcd: C 64.95, H 6.52, N 18.16, O 10.37.

4.1.2.7.21.

4-((6-methoxy-7-(3-(4-(pyridin-4-yl)piperazin-1-yl)propoxy)quinazolin-4-yl)amino)benzonitrile (**28**) Yield: 81%, m.p.:166-168□. ^{1}H NMR (400 MHz, DMSO-d_6): δ 9.78 (s, 1H, NH), 8.58 (s, 1H, ArH), 8.23 (d, 2H, ArH), 8.12 (d, *J* = 8.5 Hz, 2H, ArH), 7.84 (m, 3H, ArH), 7.23 (s, 1H, ArH), 7.09 (d, 2H, ArH), 4.22 (t, 2H, -O***CH*$_2$**CH$_2$CH$_2$N-), 3.99 (s, 3H, -OCH$_3$), 3.15–2.55 (m, 8H, -N*CH*$_2$-), 2.37 (m, 2H, -N*CH*$_2$-), 1.89 (m, 2H, -OCH$_2$***CH*$_2$**CH$_2$N-). ^{13}C NMR (100 MHz, DMSO-d_6): δ 158.76, 156.65, 156.33, 150.67, 149.89, 149.01, 148.62, 144.88, 131.14, 126.84, 113.09, 108.89, 107.34, 106.21, 102.88, 70.81, 56.06, 54.09, 53.36, 49.24, 26.68. ESI-MS: m/z calcd found 496.25 [M+H] $^{+}$. Anal. calcd: C 67.83, H 5.94, N 19.76, O 6.47.

4.1.2.7.22.

4-((6-methoxy-7-(3-morpholinopropoxy)quinazolin-4-yl)amino)benzonitrile (**29**) Yield: 78%, m.p.:276-278□. ^{1}H NMR (400 MHz, DMSO-d_6): δ 9.78 (s, 1H, NH), 8.58 (s, 1H, ArH), 8.12 (d, *J* = 8.5 Hz, 2H, ArH), 7.92-7.78 (m, 3H, ArH), 7.23 (s, 1H, ArH), 4.19 (t, 2H, -O***CH*$_2$**CH$_2$CH$_2$N-), 3.95 (s, 3H, -OCH$_3$), 3.58 (m, 4H, -O***CH*$_2$**CH$_2$-), 2.47-2.32 (m, 6H, -N*CH*$_2$-), 1.99 (m, 2H, -OCH$_2$***CH*$_2$**CH$_2$N-). ^{13}C NMR (100 MHz, DMSO-d_6): δ 158.67, 156.55, 156.09, 149.56, 148.53, 144.89, 131.05, 126.73, 113.61, 108.81, 106.09, 102.79, 69.37, 66.06, 56.86, 54.97, 54.01, 26.88. ESI-MS: m/z calcd found 419.32 [M+H] $^{+}$. Anal. calcd: C 65.88, H 6.03, N 16.68, O 11.41.

4.1.2.7.23.

3-((6-methoxy-7-(3-(pyrrolidin-1-yl)propoxy)quinazolin-4-yl)amino)benzonitrile (**30**) Yield: 79%, m.p.:172-174□. ^{1}H NMR (400 MHz, DMSO-d_6): δ 9.68 (s, 1H, NH), 8.54 (s, 1H, ArH), 8.38 (s, 1H, ArH), 8.15 (d, *J* = 8.1 Hz, 1H, ArH), 7.83 (s, 1H, ArH), 7.67-7.44 (m, 2H, ArH), 7.21 (s, 1H, ArH), 4.19 (t, 2H, -O***CH*$_2$**CH$_2$CH$_2$N-), 3.98 (s, 3H, -OCH$_3$), 2.58 (t, *J* = 7.1 Hz, 2H, -N*CH*$_2$-), 2.51 (s, 2H, -N*CH*$_2$-), 2.48 (s, 2H,

-N*CH*$_2$-), 2.04-1.93 (m, 2H, -OCH$_2$***CH*****$_2$**CH$_2$N-), 1.70 (s, 4H, -CH$_2$CH$_2$-). ^{13}C NMR (100 MHz, DMSO-*d*$_6$): δ 158.48, 156.35, 154.75, 149.86, 148.53, 147.89, 141.83, 130.05, 125.46, 119.67, 115.73, 110.61, 108.81, 106.41, 103.79, 69.87, 56.67, 54.83, 53.89, 25.86, 22.37. ESI-MS: m/z 404.30 [M+H] $^+$. Anal. calcd: C 68.44, H 6.24, N 17.38, O 7.94.

4.1.2.7.24.

3-((6-methoxy-7-(3-(piperidin-1-yl)propoxy)quinazolin-4-yl)amino)benzonitrile (**31**) Yield: 81%, m.p.:146-148□. ^{1}H NMR (400 MHz, DMSO-*d*$_6$): δ 9.67 (s, 1H, NH), 8.55 (s, 1H, ArH), 8.38 (s, 1H, ArH), 8.15 (d, *J* = 8.0 Hz, 1H, ArH), 7.83 (s, 1H, ArH), 7.65-7.52 (m, 2H, ArH), 7.21 (s, 1H, ArH), 4.18 (s, 2H, -O***CH*****$_2$**CH$_2$CH$_2$N-), 3.98 (s, 3H, -OCH$_3$), 2.48-2.41 (m, 2H, -OCH$_2$***CH*****$_2$**CH$_2$N-), 2.37 (s, 4H, -N*CH*$_2$-), 1.94 (m, 4H, -N*CH*$_2$-, -***CH*****$_2$**CH$_2$CH$_2$-), 1.56-1.48 (m, 4H, -CH$_2$CH$_2$CH$_2$-). ^{13}C NMR (100 MHz, DMSO-*d*$_6$): δ 158.53, 156.39, 154.67, 149.89, 148.65, 147.88, 141.89, 130.06, 125.56, 119.76, 115.86, 110.77, 108.89, 106.43, 103.81, 69.72, 56.37, 55.44, 54.83, 26.87, 24.45, 23.37. ESI-MS: m/z 418.38 [M+H] $^+$. Anal. calcd: C 69.03, H 6.53, N 16.74, O 7.70.

4.1.2.7.25.

3-((6-methoxy-7-(3-(4-methylpiperidin-1-yl)propoxy)quinazolin-4-yl)amino)benzonitrile (**32**) Yield: 83%, m.p.:142-144□. ^{1}H NMR (400 MHz, DMSO-*d*$_6$): δ 9.67 (s, 1H, NH), 8.54 (s, 1H, ArH), 8.38 (s, 1H, ArH), 8.15 (dd, *J* = 5.1, 4.0 Hz, 1H, ArH), 7.83 (s, 1H, ArH), 7.67-7.49 (m, 2H, ArH), 7.20 (s, 1H, ArH), 4.17 (s, 2H, -O***CH*****$_2$**CH$_2$CH$_2$N-), 3.98 (s, 3H, -OCH$_3$), 2.85 (d, *J* = 11.2 Hz, 2H, -N*CH*$_2$-), 2.53-2.50 (m, 2H, -OCH$_2$CH$_2$***CH*****$_2$**N-), 2.43 (t, *J* = 7.0 Hz, 2H, -N*CH*$_2$-), 1.93 (ddd, *J* = 28.7, 17.0, 8.2 Hz, 4H, -OCH$_2$***CH*****$_2$**CH$_2$N-, -NCH$_2$***CH*****$_2$**-), 1.57 (m, 3H, -NCH$_2$***CH*****$_2$**-, -C***H***CH$_3$), 0.88 (d, *J* = 6.5 Hz, 3H, -CH***CH*****$_3$**). ^{13}C NMR (100 MHz, DMSO-*d*$_6$): δ 158.56, 156.41, 154.69, 149.91, 148.67, 147.87, 141.84, 130.16, 125.77, 119.82, 115.86, 110.79, 108.91, 106.56, 103.87, 69.91, 56.32, 54.35, 45.87, 31.54, 30.88, 26.76, 19.43. ESI-MS: m/z 432.32 [M+H] $^+$. Anal. calcd: C 69.57, H 6.75, N 16.24, O 7.44.

4.1.2.7.26.

3-((6-methoxy-7-(3-(4-methylpiperazin-1-yl)propoxy)quinazolin-4-yl)amino)benzonitrile (**33**) Yield: 86%, m.p.:152-154□. ^{1}H NMR (400 MHz, DMSO-*d*$_6$): δ 9.67 (s, 1H, NH), 8.55 (s, 1H, ArH), 8.38 (s, 1H, ArH), 8.15 (d, *J* = 7.9 Hz, 1H, ArH), 7.83 (s, 1H, ArH), 7.76-7.45 (m, 2H, ArH), 7.20 (s, 1H, ArH), 4.18 (s, 2H, -O***CH*****$_2$**CH$_2$CH$_2$N-), 3.98 (s, 3H, -OCH$_3$), 2.51 (s, 2H, -OCH$_2$CH$_2$***CH*****$_2$**N-), 2.42 (dd, *J* = 28.5, 21.5 Hz, 8H, -N*CH*$_2$-), 2.16 (s, 3H, -NCH$_3$), 2.03-1.89 (m, 2H, -OCH$_2$***CH*****$_2$**CH$_2$N-). ^{13}C NMR (100 MHz, DMSO-*d*$_6$): δ 158.66, 156.47, 154.58, 149.84, 148.78, 147.88, 141.89, 130.26, 125.69, 119.82, 115.77, 110.83, 108.88, 106.69, 103.89, 70.86, 55.92, 54.59, 54.11, 52.36, 43.73, 25.85. ESI-MS: m/z 433.37 [M+H] $^+$. Anal. calcd: C 66.67, H 6.51, N 19.42,O 7.40.

4.1.2.7.27.

3-((7-(3-(4-ethylpiperazin-1-yl)propoxy)-6-methoxyquinazolin-4-yl)amino)benzonitrile (**34**) Yield: 83%, m.p.:142-144□. ^{1}H NMR (400 MHz, DMSO-*d*$_6$): δ 9.67 (s, 1H, NH), 8.54 (s, 1H, ArH), 8.38 (s, 1H, ArH), 8.15 (d, *J* = 8.4 Hz, 1H, ArH), 7.83 (s, 1H, ArH), 7.68-7.53 (m, 2H, ArH), 7.20 (s, 1H, ArH), 4.18 (t, *J* = 6.4 Hz, 2H,

-O***CH₂***CH_2CH_2N-), 3.98 (s, 3H, -OCH_3), 2.53-2.49 (m, 2H, -N*CH₂*-), 2.47-2.42 (m, 2H, -N***CH₂***CH_3), 2.31 (dt, *J* = 14.3, 7.2 Hz, 4H, -N*CH₂*-), 1.94 (m, 2H, -OCH_2***CH₂***CH_2N-), 0.98 (t, *J* = 7.2 Hz, 3H, -NCH_2***CH₃***). ^{13}C NMR (100 MHz, DMSO-*d₆*): δ 158.67, 156.45, 154.63, 149.89, 148.71, 147.85, 141.85, 130.21, 125.72, 119.79, 115.75, 110.81, 108.88, 106.63, 103.85, 70.85, 55.81, 54.54, 54.31, 53.29, 47.76, 25.89, 12.92. ESI-MS: m/z 447.30 $[M+H]^+$. Anal. calcd: C 67.25, H 6.78, N 18.81, O 7.16.

4.1.2.7.28.

3-((6-methoxy-7-(3-morpholinopropoxy)quinazolin-4-yl)amino)benzonitrile (**35**) Yield: 80%, m.p.:266-268□. ^{1}H NMR (400 MHz, DMSO-*d₆*): δ 9.68 (s, 1H, NH), 8.58 (s, 1H, ArH), 8.38 (s, 1H, ArH), 8.15 (d, *J* = 8.4 Hz, 1H, ArH), 7.81 (s, 1H, ArH), 7.69-7.51 (m, 2H, ArH), 7.23 (s, 1H, ArH), 4.19 (m, 2H, -O***CH₂***CH_2CH_2N-), 3.97 (s, 3H, -OCH_3), 3.59 (m, 4H, -O***CH₂***CH_2-), 2.50-2.42 (m, 6H, -N*CH₂*-), 1.99 (m, 2H, -OCH_2***CH₂***CH_2N-). ^{13}C NMR (100 MHz, DMSO-*d₆*): δ 158.67, 156.45, 154.63, 149.89, 148.71, 147.85, 141.85, 130.21, 125.72, 119.79, 115.75, 110.81, 108.88, 106.63, 103.85, 69.39, 66.84, 56.77, 54.97, 54.05, 26.92. ESI-MS: m/z calcd found 419.33 $[M+H]^+$. Anal. calcd: C 65.86, H 6.02, N 16.67, O 11.45.

4.1.2.7.29.

2-((6-methoxy-7-(3-(pyrrolidin-1-yl)propoxy)quinazolin-4-yl)amino)benzonitrile (**36**) Yield: 78%, m.p.:142-144□. ^{1}H NMR (400 MHz, DMSO-*d₆*): δ 8.46 (s, 1H, ArH), 8.06 (d, *J* = 8.7 Hz, 2H, ArH), 7.92-7.87 (m, 2H, ArH), 7.27-7.23 (m, 2H, ArH), 4.12 (m, 2H, -O***CH₂***CH_2CH_2N-), 3.81 (s, 3H, -OCH_3), 2.65-2.21 (m, 6H, -N*CH₂*-), 1.80 (m, 2H, -OCH_2***CH₂***CH_2N-), 1.60 (m, 4H, -CH_2CH_2-). ^{13}C NMR (100 MHz, DMSO-*d₆*): δ 157.97, 156.27, 155.01, 149.85, 147.49, 141.38, 133.05, 128.71, 123.36, 118.01, 115.09, 110.76, 107.34, 102.89, 102.67, 69.89, 56.72, 54.86, 53.92, 25.88, 22.37. ESI-MS: m/z calcd found 404.22 $[M+H]^+$. Anal. calcd: C 68.46, H 6.25, N 17.36, O 7.93.

4.1.2.7.30.

2-((6-methoxy-7-(3-(piperidin-1-yl)propoxy)quinazolin-4-yl)amino)benzonitrile (**37**) Yield: 80%, m.p.:156-158□. ^{1}H NMR (400 MHz, DMSO-*d₆*): δ 8.47 (s, 1H, ArH), 8.12 (d, *J* = 8.7 Hz, 1H, ArH), 8.06 (d, *J* = 8.7 Hz, 1H, ArH), 7.92 (m, 1H, ArH), 7.52 (m, 1H, ArH), 7.24 (s, 1H, ArH), 7.16 (m, 1H, ArH), 4.12 (m, 2H, -O***CH₂***CH_2CH_2N-), 3.82 (s, 3H, -OCH_3), 2.65-2.21 (m, 6H, -N*CH₂*-), 1.95 (m, 2H, -OCH_2***CH₂***CH_2N-), 1.32-1.30 (m, 6H, -$CH_2CH_2CH_2$-). ^{13}C NMR (100 MHz, DMSO-*d₆*): δ 157.89, 156.33, 155.17, 149.88, 147.53, 141.39, 133.12, 128.79, 123.43, 118.07, 115.11, 110.91, 107.45, 102.90, 102.77, 69.78, 56.43, 55.55, 54.89, 26.91, 24.54, 23.43. ESI-MS: m/z calcd found 418.24 $[M+H]^+$. Anal. calcd: C 69.04, H 6.49, N 16.75, O 7.62.

4.1.2.7.31.

2-((6-methoxy-7-(3-(4-methylpiperidin-1-yl)propoxy)quinazolin-4-yl)amino)benzonitrile (**38**) Yield: 84%, m.p.:162-164□. ^{1}H NMR (400 MHz, DMSO-*d₆*): δ 8.48 (s, 1H, ArH), 8.13 (d, *J* = 8.7 Hz, 1H, ArH), 8.06 (d, *J* = 8.04 Hz, 1H, ArH), 7.62-7.58 (m, 2H, ArH), 7.26 (s, 1H, ArH), 7.20 (s, 1H, ArH), 4.19 (m, 2H, -O***CH₂***CH_2CH_2N-), 3.82 (s, 3H, -OCH_3), 2.10 (m, 2H, -OCH_2***CH₂***CH_2N-), 1.83 (m, 2H, -NCH_2***CH₂***-), 1.37 (m, 3H, -NCH_2***CH₂***-, -***CH***CH_3), 0.74 (d, *J* = 6.5 Hz, 3H, -CH***CH₃***). ^{13}C NMR (100 MHz,

DMSO-d_6): δ 157.94, 156.43, 155.22, 149.89, 147.55, 141.42, 133.15, 128.83, 123.46, 118.14, 115.18, 110.89, 107.51, 102.77, 102.87, 69.86, 56.37, 54.39, 45.88, 31.59, 30.92, 26.83, 19.46. ESI-MS: m/z 432.25 $[M+H]^+$. Anal. calcd: C 69.56, H 6.77, N 16.23, O 7.44.

4.1.2.7.32.

2-((6-methoxy-7-(3-(4-methylpiperazin-1-yl)propoxy)quinazolin-4-yl)amino)benzonitrile (**39**) Yield: 81%, m.p.:154-157□. ^{1}H NMR (400 MHz, DMSO-d_6): δ 8.48 (s, 1H, ArH), 8.13 (d, *J* = 8.7 Hz, 1H, ArH), 8.06 (d, *J* = 8.04 Hz, 1H, ArH), 7.91 (m, 1H, ArH), 7.62-7.58 (m, 1H, ArH), 7.25 (s, 1H, ArH), 7.08 (s, 1H, ArH), 4.03 (m, 2H, -O***CH₂***CH_2CH_2N-), 3.87 (s, 3H, -OCH_3), 2.51-2.22 (m, 8H, -NCH_2-), 2.16 (s, 3H, -NCH_3), 2.08 (m, 2H, -OCH_2CH_2***CH₂***N-), 1.80 (m, 2H, -OCH_2***CH₂***CH_2N-). ^{13}C NMR (100 MHz, DMSO-d_6): δ 157.98, 156.45, 155.27, 149.91, 147.59, 141.47, 133.19, 128.87, 123.49, 118.17, 115.19, 110.89, 107.53, 102.79, 102.89, 70.92, 55.97, 54.63, 54.18, 52.38, 43.78, 25.89. ESI-MS: m/z calcd found 433.25 $[M+H]^+$. Anal. calcd: C 66.66, H 6.50, N 19.44, O 7.40.

4.1.2.7.33.

2-((7-(3-(4-ethylpiperazin-1-yl)propoxy)-6-methoxyquinazolin-4-yl)amino)benzonitrile (**40**) Yield: 83%, m.p.:160-163□. ^{1}H NMR (400 MHz, DMSO-d_6): δ 8.48 (s, 1H, ArH), 8.13 (d, *J* = 8.7 Hz, 1H, ArH), 8.06 (d, *J* = 8.04 Hz, 1H, ArH), 7.91 (m, 1H, ArH), 7.62-7.58 (m, 1H, ArH), 7.25 (s, 1H, ArH), 7.08 (s, 1H, ArH), 4.03 (m, 2H, -O***CH₂***CH_2CH_2N-), 3.87 (s, 3H, -OCH_3), 2.51-2.22 (m, 8H, -NCH_2-), 2.16 (s, 3H, -N***CH₂***CH_3), 2.08 (m, 2H, -OCH_2CH_2***CH₂***N-), 1.80 (m, 2H, -OCH_2***CH₂***CH_2N-), 0.94 (t, *J* = 6.52 Hz, 3H, -NCH_2***CH₃***). ^{13}C NMR (100 MHz, DMSO-d_6): δ 157.97, 156.46, 155.26, 149.89, 147.59, 141.49, 133.21, 128.88, 123.51, 118.21, 115.23, 110.88, 107.57, 102.82, 102.88, 70.84, 55.87, 54.56, 54.37, 53.32, 47.77, 25.89, 12.93. ESI-MS: m/z calcd found 447.26 $[M+H]^+$. Anal. calcd: C 67.26, H 6.77, N 18.82, O 7.15.

4.1.2.7.34.

2-((6-methoxy-7-(3-morpholinopropoxy)quinazolin-4-yl)amino)benzonitrile (**41**) Yield: 81%, m.p.:272-274□. ^{1}H NMR (400 MHz, DMSO-d_6): δ 8.48 (s, 1H, ArH), 8.13 (d, *J* = 8.7 Hz, 1H, ArH), 8.06 (d, *J* = 8.7 Hz, 1H, ArH), 7.91 (m, 1H, ArH), 7.52 (m, 1H, ArH), 7.23 (s, 1H, ArH), 7.16 (m, 1H, ArH), 4.11 (m, 2H, -O***CH₂***CH_2CH_2N-), 3.87 (s, 3H, -OCH_3), 3.64-3.58 (m, 4H, -O***CH₂***CH_2-), 2.54-2.42 (m, 6H, -NCH_2-), 1.98 (m, 2H, -OCH_2***CH₂***CH_2N-). ^{13}C NMR (100 MHz, DMSO-d_6): δ 157.97, 156.49, 155.27, 149.92, 147.57, 141.53, 133.24, 128.89, 123.48, 118.19, 115.26, 110.89, 107.60, 102.87, 102.92, 69.46, 66.87, 56.87, 54.93, 54.12, 26.89. ESI-MS: m/z calcd found 419.34$[M+H]^+$. Anal. calcd: C 65.85, H 6.03, N 16.68, O 11.44.

4.2. Biochemical and biological assays

4.2.1. Cell lines culture and treatments

Human liver cancer cell line (HepG2), human lung carcinoma cell line (A549), human breast carcinoma cell line (MCF-7), human prostate cancer cell line (DU145), human neuroblastoma cancer cell line (SH-SY5Y) and human normal cell line (CCC-HPF-1) were purchased from Cancer Hospital, Chinese Academy of Medical Sciences, Beijing, P. R. China. All the cells were cultivated in DMEM/High Glucose

(4.5 g/L glucose) medium or RPMI-1640 medium supplemented with 10% fetal bovine serum (FBS), 4 mM glutamine, 50 units/mL of penicillin and 50 μg/mL of streptomycin. All cell lines were routinely maintained at 37□ in a humidified incubator with 5% CO_2 and 95% air.

4.2.2. *In vitro* anti-proliferative activities screening of target compounds assay

The anti-proliferative activities of all target compounds were determined using a standard MTT-based colorimetric assay. For a typical screening experiment to determine the cell proliferation, the tested cells were seeded in costar 96-well cell culture clusters at a density of 2×10^3 cells/well in 100 μL of the proper culture medium and performed of incubation at 37□ with 5% CO_2. After 24 h incubation period，the medium was removed and the cells were treated with the indicated concentrations of target compounds (0.1-100 μM) in 100 μL for 72 h. 100 μL of fresh medium without cells was added as control. Triplicate wells were prepared for each individual dose. After that, the cells were incubated with 10 μL MTT solution (5 mg/mL in PBS) for a further 4 h and then 100 μL of 10% SDS (w/v) with NH_4Cl (1 mg/ml) was added to each well. The plates were kept for 10 h at 37℃ with 5% CO_2. The purple color was produced. The absorbance of formazan was measured on a BioTek microtiter plate reader at 570 nm with correction at 650 nm. At least three independent experiments were performed. Survival ratios are expressed in percentages with respect to untreated cells. The percent growth inhibition was calculated by the following formula: $\%inhibition=[1-(OD_{treated}-OD_{blank})/(OD_{control}-OD_{blank})]\times100$. Then IC_{50} values were calculated from the above data with SPSS16.0 software. The results were then represented as obtained after averaging at least thrice independent experiments.

4.2.3. EGFR-TK binding inhibitory assay

The EGFR kinase assay was performed in order to determine the ability of compound **21** to block the tyrosine kinase activity of EGFR-TK. Costar 96-well cell culture clusters were pre-coated with 100 μL/well of 10 μg/mL streptavidin in carbonate buffer at 4°C for 10 h. After the excess streptavidin solution was removed by washing the wells thrice with wash buffer (0.05% Tween-20 in PBS). An aliquot of solution (H_2O/DMSO:99/1,v/v) (15 μL) containing various concentrations of a screened inhibitor compound **21** was added to 15 μL DTT/kinase buffer (pH 7.5, CST) containing 200 ng/μL EGFR-TK (Sino Biological Inc.), and then incubated at room temperature (25℃) for 5 min, followed by addition of 30 μL mixed solution containing 15 μL PTP1B (Tyr66) biotinylated peptide (CST), 1.2 μL ATP (CST) and 13.8 μL ultra-pure H_2O. The resulting mixture was left for reaction at 37℃ for 1 h, and then added 60 μL stop buffer (50 mM EDTA, pH 8.0, CST) to stop the reaction. 25 μL/well of each enzymatic reaction mixture and 75 μL/well of ultra-pure H_2O were transferred to a 96-well streptavidin-coated cell culture cluster and incubated at 37℃ for 1 h. Following thrice of washing with PBS/T, 100 μL of primary antibody (Phospho-Tyrosine Mouse mAb, 1:1000 in PBS/T with 1.5% BSA) was added to each well and the plate was incubated at 37℃ for another 1 h. The plate was again washed thrice with PBS/T, and then 100 μL of secondary antibody (HRP-labeled Goat Anti-Mouse IgG, 1:1000 in PBS/T with 1.5% BSA) was added to each well for 1 h of

incubation at 37□, followed by thrice of washing with PBS/T. 100 μL of TMB substrate system was added to each well and the plate was incubated at 37□ for 15 min, and then the reaction was stopped by addition of 100 μL of 1 M H_2SO4, and the plate was read on the ELISA plate reader at 450 nm with correction at 650 nm. The results were expressed as percent kinase activity of the vehicle control, and the IC_{50} value was defined as the compound concentration that resulted in 50% inhibition of enzyme activity. The kinase assay was performed at least thrice independently.

4.2.4. LDH release assay

1.0×10^5 cells per well HepG2 cells were inoculated into a costar 24-well cell culture cluster and incubated for 24 h at 37□ in 5% CO_2. Cytotoxicity was assessed based on measuring the LDH release after 48 h of various dose compound **21** treatments. Prior to each assay, the cells were lysed with 2% (V/V) lysate in culture media for 1 h at 37□ to obtain a representative maximal LDH release as the positive control with 100% cytotoxicity and the cells in culture medium alone was the low control. The amounts of LDH in the supernatant were determined on a BioTek microtiter plate reader and calculated as kit instructions. All tests were performed in triplicate and the assay was repeated three times independently.

4.2.5. Flow cytometric analysis of cell cycle distribution assay

For flow cytometric analysis of DNA content, 5.0×10^5 cell/well HepG2 cells were grown in a costar 6-well cell culture cluster and grown for 24 h at 37□ in 5%CO_2, after the medium was removed and the cells were treated with different concentrations of the test compound **21** for 48 h. Blank wells treated with medium only were also included. After the incubation period, the HepG2 cells were collected, washed twice with ice-cold PBS, centrifuged and then fixed with ice-cold ethanol (70%) for at least 24 h. Cells were then collected, washed twice with ice-cold PBS, and treated with 30 μL RNase A (1 mg/ml) in PBS at 37□ for about 30 min, and then stained with 50 μL propidium iodide (50 mg/mL) in PBS, the staining process lasted 30 min at 4□ in darkness. The cellular DNA content of the stained cells was then analyzed on BD-FACS Aria □ flow cytometer and the cell cycle distribution was quantified.

4.2.6. Analysis of apoptosis induced in HepG2 cells

The HepG2 cells were seeded in a costar 6-well cell culture cluster at a seeding density of 5.0×10^5 cells/mL and incubated for 24 h. When the cells were adhered, various concentrations of compound **21** were added. The cells were treated with compound **21** for 48 h and then collected, washed twice with ice-cold PBS, and cell apoptosis was analyzed using AnnexinV-FITC (5 μL) and propidium iodide (5 μL) double staining on BD-FACS Aria □ flow cytometer. Early apoptotic cells were defined as AnnexinV-FITC positive/PI negative, late apoptotic cells as AnnexinV-FITC/PI double positive and necrotic cells as AnnexinV-FITC positive/PI positive.

4.2.7. Morphological observation of HepG2 cells

Furthermore, dramatic alterations in the morphology of HepG2 cells were observed by Hoechst 33342/propidium iodide dual staining under fluorescence microscopy to determine whether the growth inhibitory activity of the selected compound **21** was related to apoptosis induction. The HepG2 cells were cultivated in a costar 6-well cell

culture cluster (5.0×10^4 cells per well) and maintained in DMEM medium with 10% FBS at 37□ for 24 h. After the cells attachment, the medium was replaced with new medium containing varying concentrations of tested drugs. After 48 h treatment, the medium was removed and the cells was washed twice with ice-cold PBS and then stained with 1:1 ratio of Hoechst 33342/propidium iodide mixture at 37□ for 30 min in the darkness. The cells were washed with ice-cold PBS thrice. Stained cells of the morphological observation was visualized using inverted the laser scanning confocal microscope at 200× magnification.

4.2.8. Effect of compound **21** on mitochondrial membrane potential assay

Changes in mitochondrial membrane potential as a result of mitochondrial perturbation were measured by staining with Rhodamine-123. The HepG2 cells were inoculated in a costar 6-well cell culture cluster at a concentration of 5.0×10^5 cells/mL and incubated with compound **21** at indicated concentrations for 48 h when all the cells were adhered. After the cells were collected, washed with ice-cold PBS twice and 500 μL Rhodamine-123 solution (5μg/mL) was added for 30 min before termination of experiment. The HepG2 cells were trypsinized, collected, washed twice with ice-cold PBS and resuspended in PBS. The fluorescence intensity of mitochondrial membrane potential was measured in FL-1 channel vs counts on BD-FACS Aria □ flow cytometer.

4.2.9. Determination of intracellular free Ca^{2+} using Fluo-3/AM assay

The HepG2 cells of 5.0×10^5 cells/mL were seeded in a costar 6-well cell culture cluster and cultured for 24 h at 37□ in 5% CO_2. After then the medium was removed and the cells were incubated with compound **21** at indicated concentrations for 48 h. After the cells were collected, washed with ice-cold PBS twice and the fluorescence Ca^{2+} indicator Fluo-3/AM solution (4 μM) was added for 30 min before termination of experiment. The HepG2 cells were trypsinized, collected, washed twice with HEPES and then resuspended in HEPES. The fluorescence intensity was measured in FL-1 channel vs counts on BD-FACS Aria □ flow cytometer.

4.2.10. Detection of intracellular reactive oxygen species (ROS) assay

The HepG2 cells of 5.0×10^5 cells/mL were grown in a costar 6-well cell culture cluster and maintained for 24 h at 37□ in 5% CO_2. After then the medium was removed and the cells were treated with compound **21** at indicated concentrations for 48 h. After the cells were collected, washed with ice-cold PBS twice and 1000 μL DCFH-DA working solution (10 μM) was added at 37□ for 30 min before termination of experiment. The HepG2 cells were trypsinized, collected, washed twice with ice-cold HBSS and resuspended in HBSS, the fluorescence was directly recorded on FS5 fluorescence spectrometer.

4.2.11. Determination of caspase-3 activation assay

Caspase-3 activation in HepG2 cells treated with compound **21** at different doses was determined following the instructions of caspase-3 activation colorimetric assay kit (KeyGEN BioTECH). 48 h after treatment, the HepG2 cells were collected, rinsed with ice-cold PBS and then lysed using lysis buffer contained 1% DTT on ice bath for 1-1.5 h. The cell lysate was centrifuged (10,000×g, 1 min, 4□), and then the supernatant were collected. Protein concentration in the supernatant was measured by

Bradford protein quantitation assay. Finally, 50 μL of the supernatant and 50 μL of the 2×Reaction Buffer containing 1% DTT, and 5 μL of caspase-3 substrate were added to each well on a costar 96-well cell culture cluster and the cluster was maintained for 4 h at 37□ in 5% CO_2. The absorbance was measured at 405 nm on a BioTek microtiter plate reader.

4.2.12. Statistical analysis

All the statistical analyses were performed under SPSS16.0 software by a personal computer. Each experiment was performed in triplicate, and all experiments were run three times independently. Measurements from all the replicates were combined and treatment effects analyzed. Unless otherwise indicated, the results are presented as the mean ± SD. The differences between different treatments were analyzed using the two-sided Student's t test. P values of less than 0.05 or 0.01 were considered significant or highly significant difference.

Acknowledgments

This work was supported by National Natural Science Foundation of China (No. 21071022) and the Fundamental Research Funds for the Central Universities. We especially thank Huabei Zhang (Key Laboratory of Radiopharmaceuticals, Ministry of Education, College of Chemistry, Beijing Normal University) for their kind help in this paper.

References

[1] S. Singhal, B.S. Chakraborty, Signal Detection of Docetaxel in Canadian Spontaneous Adverse Event Reports, J. Pharm. Res., (2012), Vol. 5, Issue 2, 1070.

[2] G.F. Macri, A. Greco, A. Gallo, M. Fusconi, M.D. Caterina Marinelli, M.D. Vincentiis, Use of electrochemotherapy in a case of neck skin metastasis of oral squamous cell carcinoma: Case report and considerations, Head & Neck, 36 (2014) E86-E90.

[3] M. Mubeen, S.G. Kini, A Review on: The Design and Development of EGFR Tyrosine Kinase Inhibitors in Cancer Therapy, Int. J. Ther. Appl., 5(2012)29-37.

[4] C. Com, Targeted Cancer Therapies : Answers to Your Questions, Targeted Cancer Therapies Answers to Your Questions. Source: www.cancer.gov.

[5] Y. Kawakita, K. Miwa, M. Seto, H. Banno, Y. Ohta, T. Tamura, T. Yusa, H. Miki, H. Kamiguchi, Y. Ikeda, T. Tanaka, K. Kamiyama, T. Ishikawa, Design and synthesis of pyrrolo[3,2-d]pyrimidine HER2/EGFR dual inhibitors: Improvement of the physicochemical and pharmacokinetic profiles for potent in vivo anti-tumor efficacy, Bioorg. Med. Chem., 20 (2012) 6171-6180.

[6] Y.S. Min, O.Y. Kee, K.J. Heon, P.M. Ja, S.I. Ock, K. Kang, G. Chai, The Modulation of Radiosensitivity by Combined Treatment of Selective COX-2 Inhibitor, NS 398 and EGF Receptor Blocker AG 1478 in HeLa Cell Line, J. Korean Soc.Ther. Radiol. Oncol., 2005;23(1): 51-60.

[7] R. Wuerstlein, I. Bauerfeind, Tumor-Specific Systemic Treatment in Advanced Breast Cancer - How Long does it Make Sense?, Breast Care, 6 (2011) 35-41.
[8] J.D. Jordan, E.M. Landau, R. Iyengar, Signaling Networks : The Origins of Cellular Multitasking, Cell, 103 (2000) 193-200.
[9] P. Blume-Jensen, T. Hunter, Oncogenic kinase signaling, Nature, 411 (2001) 355-365.
[10] T. Ishikawa, M. Seto, H. Banno, Y. Kawakita, M. Oorui, T. Taniguchi, Y. Ohta, T. Tamura, A. Nakayama, H. Miki, Design and synthesis of novel human epidermal growth factor receptor 2 (HER2)/epidermal growth factor receptor (EGFR) dual inhibitors bearing a pyrrolo[3,2-d]pyrimidine scaffold, J. Med. Chem., 54 (2011) 8030-8050.
[11] L. Shuang, Z. Wei, L. Ji, Q. Luo, H. Xiang, X. Li, F. Wang, Synthesis, characterization, screening and docking analysis of4-anilinoquinazoline derivatives as tyrosine kinase inhibitors, Eur. J. Med. Chem., 61 (2013) 84-94.
[12] S. Bishayee, Role of conformational alteration in the epidermal growth factor receptor (EGFR) function, Biochem. Pharmacol., 60 (2000) 1217-1223.
[13] A. Chilin, M.T. Conconi, G. Marzaro, A. Guiotto, L. Urbani, F. Tonus, P. Parnigotto, Exploring epidermal growth factor receptor (EGFR) inhibitor features: the role of fused dioxygenated rings on the quinazoline scaffold, J. Med. Chem., 53 (2010) 1862-1866.
[14] C.H. Yun, T.J. Boggon, Y. Li, M.S. Woo, H. Greulich, M. Meyerson, M.J. Eck, Structures of Lung Cancer-Derived EGFR Mutants and Inhibitor Complexes: Mechanism of Activation and Insights into Differential Inhibitor Sensitivity, Cancer Cell, 11 (2007) 217-227.
[15] M.S.A. Elsayed, M.E. El-Araby, R.A.T. Serya, A.H. El-Khatib, M.W. Linscheid, K.A.M. Abouzid, Structure-based design and synthesis of novel pseudosaccharine derivatives as antiproliferative agents and kinase inhibitors, Eur. J. Med. Chem., 61 (2013) 122–131.
[16] T. Holbro, G. Civenni, N.E. Hynes, The ErbB receptors and their role in cancer progression, Exp. Cell Res., 284 (2003) 99-110.
[17] A. Garofalo, L. Goossens, B. Baldeyrou, A. Lemoine, S. Ravez, P. Six, M. Davidcordonnier, J.P. Bonte, P. Depreux, A. Lansiaux, Design, Synthesis, and DNA-Binding of N-Alkyl(anilino)quinazoline Derivatives, J. Med. Chem., 53 (2010) 8089-8103.
[18] Z. Feng, Z. Lin, W. Feng, W. Zhao, X. Dong, Four-membered heterocycles-containing 4-anilino-quinazoline derivatives as epidermal growth factor receptor (EGFR) kinase inhibitors, Bioorg. Med. Chem. Lett., 23 (2013) 5385-5388.
[19] H. Ogiso, R. Ishitani, O. Nureki, S. Fukai, M. Yamanaka, J.H. Kim, K. Saito, A. Sakamoto, M. Inoue, M. Shirouzu, Crystal Structure of the Complex of Human Epidermal Growth Factor and Receptor Extracellular Domains, Cell, 110 (2002) 775-787.
[20] S. Li, X. Wang, Y. He, M. Zhao, Y. Chen, J. Xu, M. Feng, J. Chang, H. Ning, C. Qi, Design and synthesis of novel quinazoline nitrogen mustard derivatives as potential therapeutic agents for cancer, Eur. J. Med. Chem., 67 (2013) 293-301.

ACCEPTED MANUSCRIPT

[21] X. Wu, M. Li, Y. Qu, W. Tang, Y. Zheng, J. Lian, M. Ji, L. Xu, Design and synthesis of novel Gefitinib analogues with improved anti-tumor activity, Bioorg. Med. Chem., 18 (2010) 3812-3822.
[22] J. Cai, L. Li, K.H. Hong, X. Wu, J. Chen, P. Wang, M. Cao, X. Zong, M. Ji, Discovery of 4-aminoquinazoline—urea derivatives as Aurora kinase inhibitors with antiproliferative activity, Bioorg. Med. Chem., 22 (2014) 5813-5823.

ACCEPTED MANUSCRIPT

Table 1
Chemical structures of the target compounds 8-41.

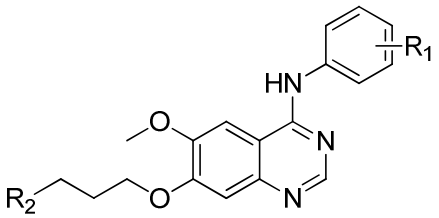

Cpd. No	R_1	R_2	Yield (%)
8	4-CN		88
9	4-CN	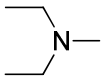	90
10	4-CN	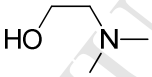	83
11	4-CN	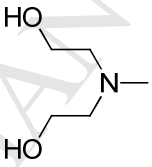	73
12	4-CN	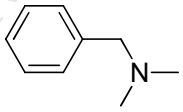	84
13	4-CN	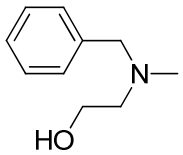	87
14	4-CN	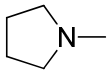	83
15	4-CN	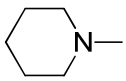	81
16	4-CN	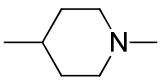	85
17	4-CN	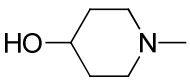	82
18	4-CN	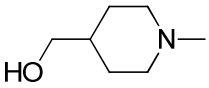	87

ACCEPTED MANUSCRIPT

19	4-CN	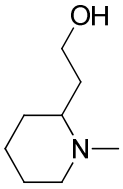	84
20	4-CN	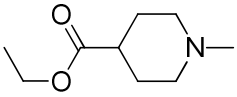	80
21	4-CN	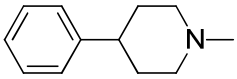	82
22	4-CN	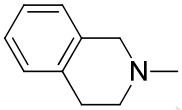	81
23	4-CN	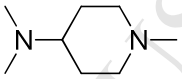	79
24	4-CN	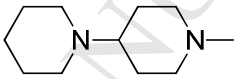	85
25	4-CN	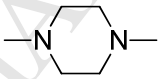	83
26	4-CN	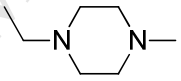	81
27	4-CN	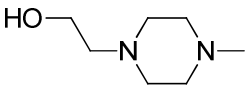	80
28	4-CN	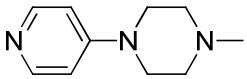	81
29	4-CN	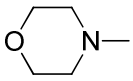	78
30	3-CN	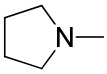	79
31	3-CN	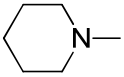	81
32	3-CN	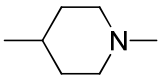	83
33	3-CN	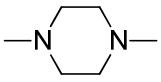	86
34	3-CN	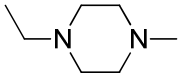	83

ACCEPTED MANUSCRIPT

35	3-CN	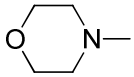	80
36	2-CN	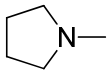	78
37	2-CN	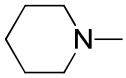	80
38	2-CN	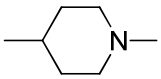	84
39	2-CN	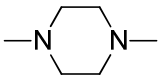	81
40	2-CN	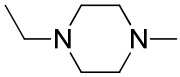	83
41	2-CN	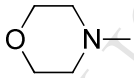	81

Table 2

In vitro anti-proliferative activities against different cancer cell lines for 72 h of the target compounds.

Cpd.	Anti-proliferative activities in different cancer cell lines (IC_{50}, μM) [a]				
	HepG2	A549	DU145	MCF-7	SH-SY5Y
8	> 100	60.52	35.25	45.01	34.88
9	59.42	50.61	68.94	> 100	> 100
10	45.24	29.03	17.36	41.41	83.67
11	40.33	26.07	20.19	36.83	48.12
12	> 100	> 100	> 100	> 100	> 100
13	> 100	47.36	> 100	> 100	> 100
14	20.88	21.77	14.38	16.24	**8.08**
15	20.69	23.53	24.41	35.11	18.76
16	32.13	32.31	16.55	43.09	**7.90**
17	67.87	29.94	74.93	> 100	> 100
18	61.80	> 100	53.21	35.08	21.62
19	> 100	> 100	> 100	> 100	> 100
20	57.69	89.86	52.29	34.89	47.21
21	**4.61**	**9.50**	**6.79**	**9.80**	**7.77**

ACCEPTED MANUSCRIPT

22	> 100	> 100	> 100	> 100	> 100
23	33.56	42.43	28.32	31.03	24.27
24	**8.84**	30.66	15.64	19.62	**9.81**
25	13.84	48.82	46.47	71.06	12.97
26	**9.58**	15.97	34.40	29.90	**5.44**
27	28.05	**9.82**	29.26	25.18	36.82
28	12.57	25.45	22.86	22.87	31.61
29	**0.77**	59.38	98.25	> 100	> 100
30	18.20	39.89	19.09	33.88	10.56
31	29.50	36.98	29.13	44.79	11.18
32	18.20	18.71	17.68	24.39	**7.33**
33	18.28	27.66	12.12	23.14	**6.89**
34	13.69	18.74	18.22	19.95	**6.27**
35	**1.89**	65.46	77.81	> 100	> 100
36	24.50	21.77	18.65	16.17	28.92
37	14.19	14.70	15.28	15.19	13.40
38	**4.03**	22.71	11.91	31.94	28.97
39	26.38	23.40	19.41	17.84	32.38
40	**2.11**	**6.91**	**5.87**	**9.07**	12.58
41	**3.68**	46.76	68.54	98.40	> 100
Gefitinib	29.79	12.08	**8.63**	12.05	18.21
QWL-22b	**3.06**	**6.71**	20.04	10.54	**8.60**

[a] The IC_{50} values are reported as means of at least three independent experiments, and SD < 10%. > 100 μM is expressed as inactive.

Table 3
The inhibition rate of cell proliferation in HepG2 cells treated with different concentrations of target compound **21** at different times.

Conc./μM	Inhibition (Mean ± SD, n = 3) [a]		
	24 h	48 h	72 h
0.1	0.044±0.052	0.057±0.055	0.074±0.115
1	0.079±0.351	0.086±0.031	0.137±0.027
10	0.635±0.241	0.556±0.254	0.636±0.023

50	0.991±0.013	1.079±0.016	0.965±0.014
100	1.009±0.019	1.023±0.008	1.013±0.035

[a] Data are expressed as mean ± SD of three independent experiments. Significant differences between groups were considered statistically significant at $^{*}P < 0.05$.

Table 4
The inhibitory rate of cell proliferation in A549 cells treated with different concentrations of target compound **21** at different times.

Conc./μM	Inhibition (Mean ± SD, n = 3) [a]		
	24 h	48 h	72 h
0.1	0.008±0.023	0.013±0.032	0.050±0.040
1	0.019±0.053	0.029±0.063	0.015±0.038
10	0.247±0.167	0.135±0.058	0.341±0.059
50	0.853±0.014	0.755±0.013	0.866±0.014
100	0.918±0.008	0.914±0.008	0.955±0.004

[a] Data are expressed as mean ± SD of three independent experiments. Significant differences between groups were considered statistically significant at $^{*}P < 0.05$.

Table 5
The IC_{50} values for 24 h, 48 h and 72 h exposure of tumor cell lines of compound **21**.

Cpd.	IC_{50} (μM) against tumor cell lines [a]					
	HepG2 cells			A549 cells		
	24 h	48 h	72 h	24 h	48 h	72 h
21	13.02	9.56	4.61	15.02	20.60	9.50

[a] The IC_{50} values are reported as means of at least three independent experiments, and SD < 10%.

Table 6
The selectivities of compound **21** and Gefitinib against tested cell lines treated with different concentrations for 72 h.

Cpd.	IC_{50} (μM) against cell lines for 72 h [a]	
	CCC-HPF-1 cells	A549 cells

21	27.97	9.50
Gefitinib	30.78	14.08

[a] The IC_{50} values are reported as means of at least three independent experiments, and SD < 10%.

Table 7
EGFR-TK inhibitory activities of compound **21** and Gefitinib treated with different concentrations *in vitro*.

Treatment	Conc./μM	OD values [a]		Inhibition/%	
		23	Gefitinib	23	Gefitinib
EGFR-TK group		0.278	0.278		
NC group		0.172	0.172		
Drug groups	0.000001	0.261	0.277	16.04	0.94
	0.00001	0.259	0.275	17.92	3.30
	0.0001	0.237	0.248	39.15	28.30
	0.001	0.229	0.219	46.23	55.66
	0.01	0.213	0.207	61.79	66.98
	0.1	0.201	0.196	73.11	77.36
	1	0.178	0.184	94.34	88.68
	10	0.173	0.169	99.06	99.83

[a] OD values are the average of at least three independent experiments run in triplicate. Variation is generally 5%.

Table 8
The IC_{50} values of EGFR-TK inhibitory activity *in vitro*.

Cpd.	IC_{50} (nM) [a]
21	3.62
Gefitinib	2.21

[a] The IC_{50} values are represented as the means of the data obtained from three separate experiments. Variation is generally 5%.

Table 9
The cell cytotoxicity of tested compounds on HepG2 cells by LDH release at varying concentrations for 48 h.

Conc./μM	Cell cytotoxicity/% [a]	
	21	Gefitinib
2.5	39.65±0.7	42.08±2.8
5.0	50.11±7.2	48.69±3.7
10.0	69.27±8.2	45.36±3.6
20.0	52.94±7.8	45.24±3.8
40.0	41.17±2.1	47.62±3.3
Natural release	37.44±2.3	37.98±5.0
Full release	100	100

[a] Data are expressed as the means of at least three independent experiments run in triplicate. Significant differences between groups were considered statistically significant at $^{*}P < 0.05$.

Table 10

Analysis of cell cycle on HepG2 cells treated at varying concentrations of compound **21** for 48 h by flow cytometry.

Conc./μM	G0/G1 (%)	S (%)	G2/M (%) [a]
NC	69.40	21.46	9.13
2.5	67.07	22.44	10.49
5.0	65.53	25.10	9.37
10.0	60.72	29.72	9.57

[a] The data are present as the average of at least three independent experiments.

Table 11

Apoptotic rates of HepG2 cells treated with compound **21** for 48 h detected by FCM.

Conc./μM	Normal/%	Early Apoptosis%	Late Apoptosis/%	Total Apoptosis/% [a]
NC	86.4	8.7	4.8	13.5
2.5	47.5	48.6	3.8	52.4
5.0	17.3	80.7	2.0	82.7
10.0	1.3	98.6	0.1	98.7

[a] The data are present as the average of at least three independent experiments.

Table 12
The changes of MMP in HepG2 cells treated with various concentrations of compound **21** for 48 h.

Group	Conc./μM	MMP/% [a]
Control		90.4
Drug treatment	2.5	88.3
	5.0	87.0
	10.0	84.0
	20.0	55.9

[a] The data are present as the average of at least three independent experiments.

Table 13
The changes of intracellular Ca^{2+} level in HepG2 cells treated with various concentrations of compound **21** for 48 h.

Group	Conc./μM	Calcium content/% [a]
Control		14.2
Drug treatment	2.5	41.7
	5.0	43.2
	10.0	48.9
	20.0	52.7

[a] The data are present as the average of at least three independent experiments.

Table 14
The activities of caspase-3 in HepG2 cells treated with various concentrations of compound **21** for 48 h.

Group	Dose/μM	OD_{405} [a]	OD_{405}/OD_{NC}
NC		0.125	100.000
Treatment groups	2.5	0.173	138.316
	5.0	0.181	145.205
	10.0	0.247	198.131
	20.0	0.245	196.479

[a] The data are present as the average of at least three independent experiments.

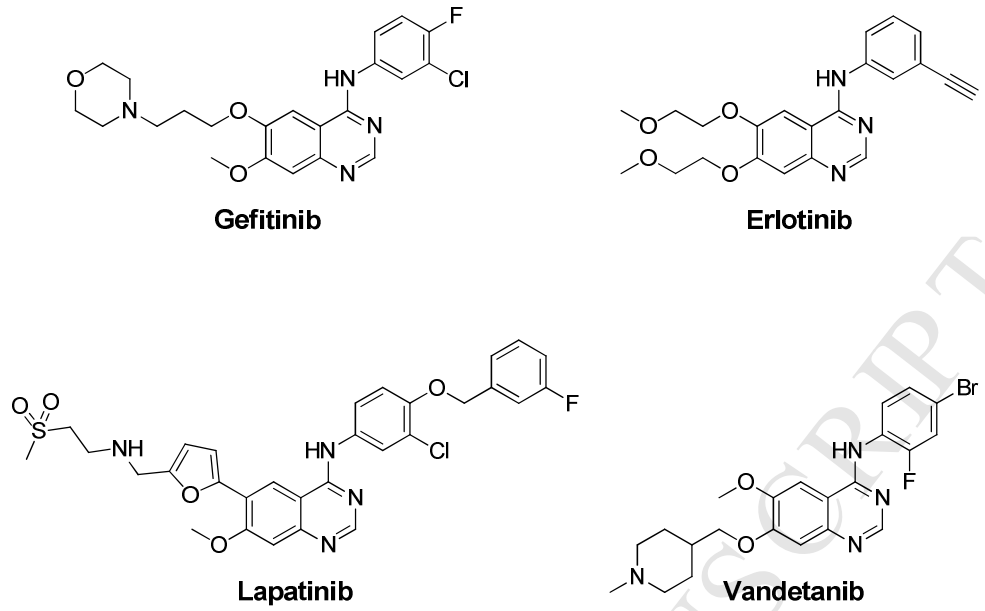

Fig. 1 The chemical structures of several small molecule EGFR inhibitors based on 4-anilinoquinazoline in clinical.

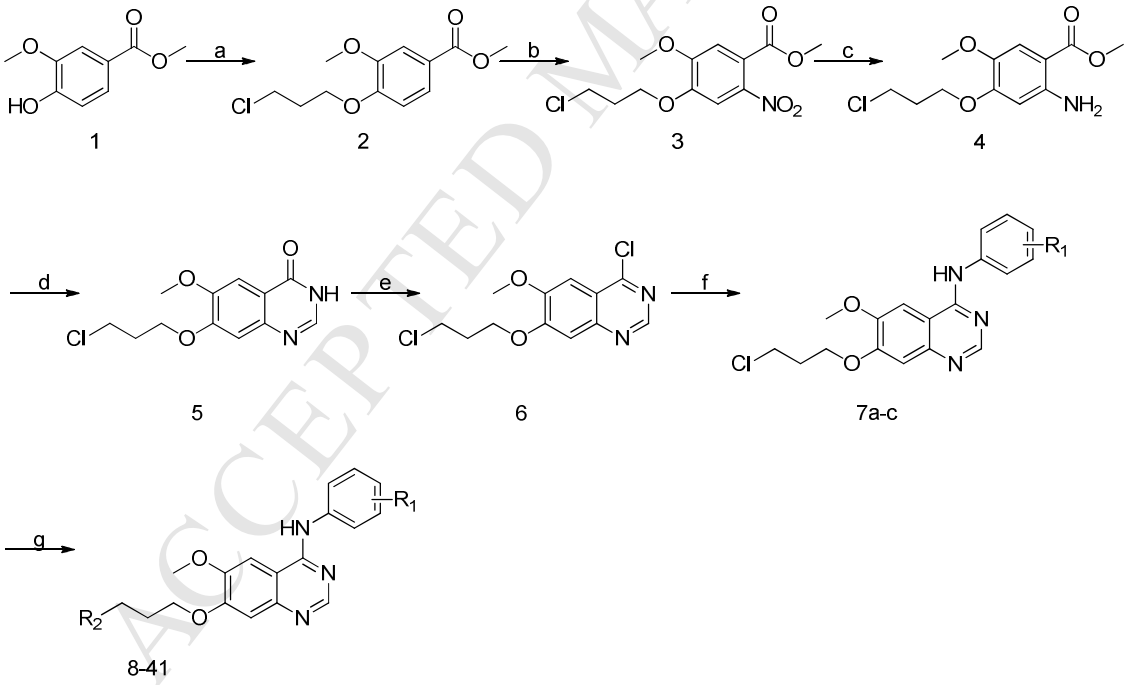

Scheme 1 General synthesis of title compounds. Reagents and conditions: a) K_2CO_3, 1-bromo-3-chloropropane, DMF, 70□,4 h; b) HNO_3, AcOH, 40□,4 h; c) Fe, AcOH, 80□,40 min; d) formamidine acetate, EtOH, reflux, 6 h; e) $POCl_3$, 105-110□,5 h; f) isopropanol, 2-/3-/4-aminobenzonitrile, reflux, 3 h; g) DMF, K_2CO_3, aliphatic amine, 60-80□, 6-10 h.

ACCEPTED MANUSCRIPT

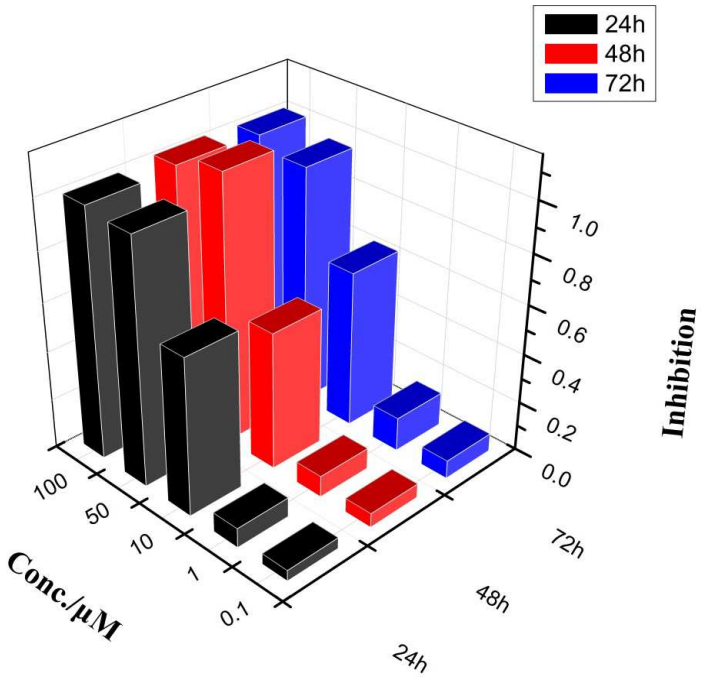

Fig. 2 Statistical results of the cell proliferation inhibition in HepG2 cells treated with different concentrations of target compound **21** at the indicated times. Points are expressed as mean ± SD of triplicate determinations.

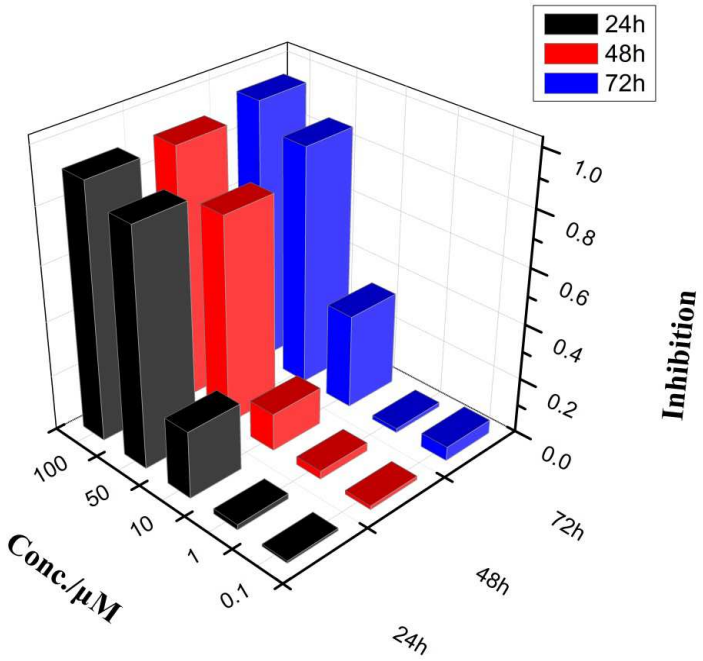

Fig. 3 Statistical results of the cell proliferation inhibition in A549 cells treated with different concentrations of target compound **21** at the indicated times. Points are expressed as mean ± SD of triplicate determinations.

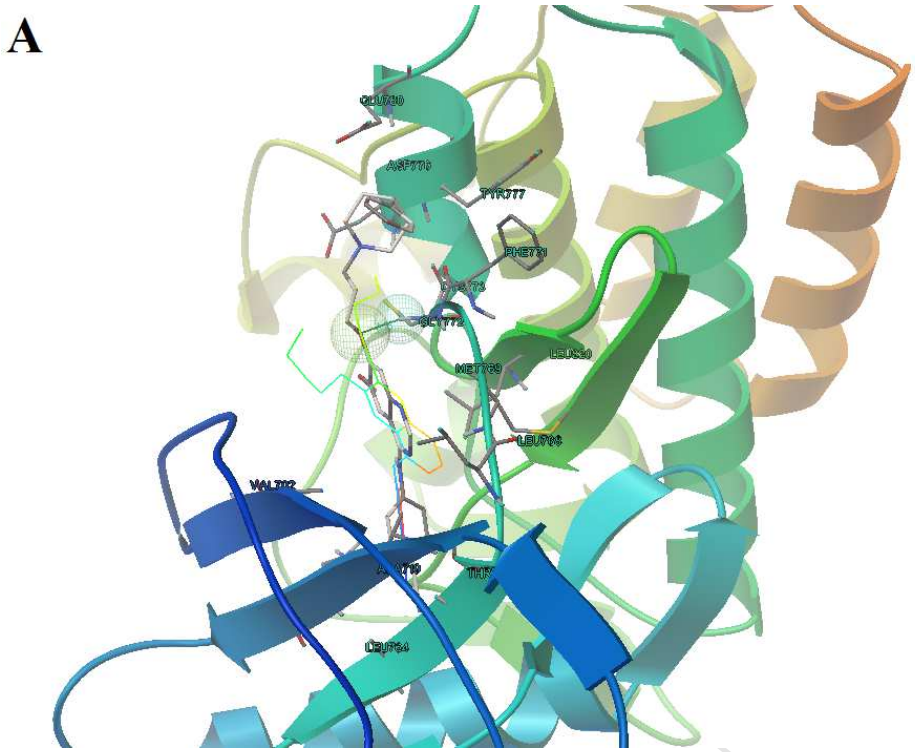
A
GLU730
ASP776
TYR777
PHE771
GLY772
LEU820
MET769
LEU768
VAL702
THR
LEU724

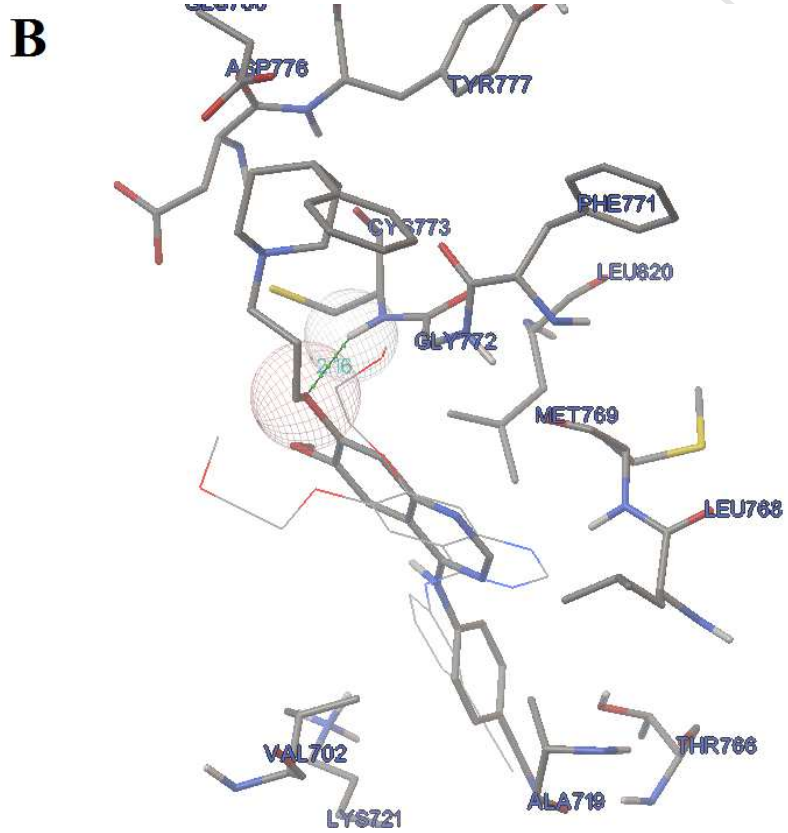
B
ASP776
TYR777
PHE771
CYS773
LEU820
GLY772
MET769
LEU768
VAL702
LYS721
ALA719
THR766

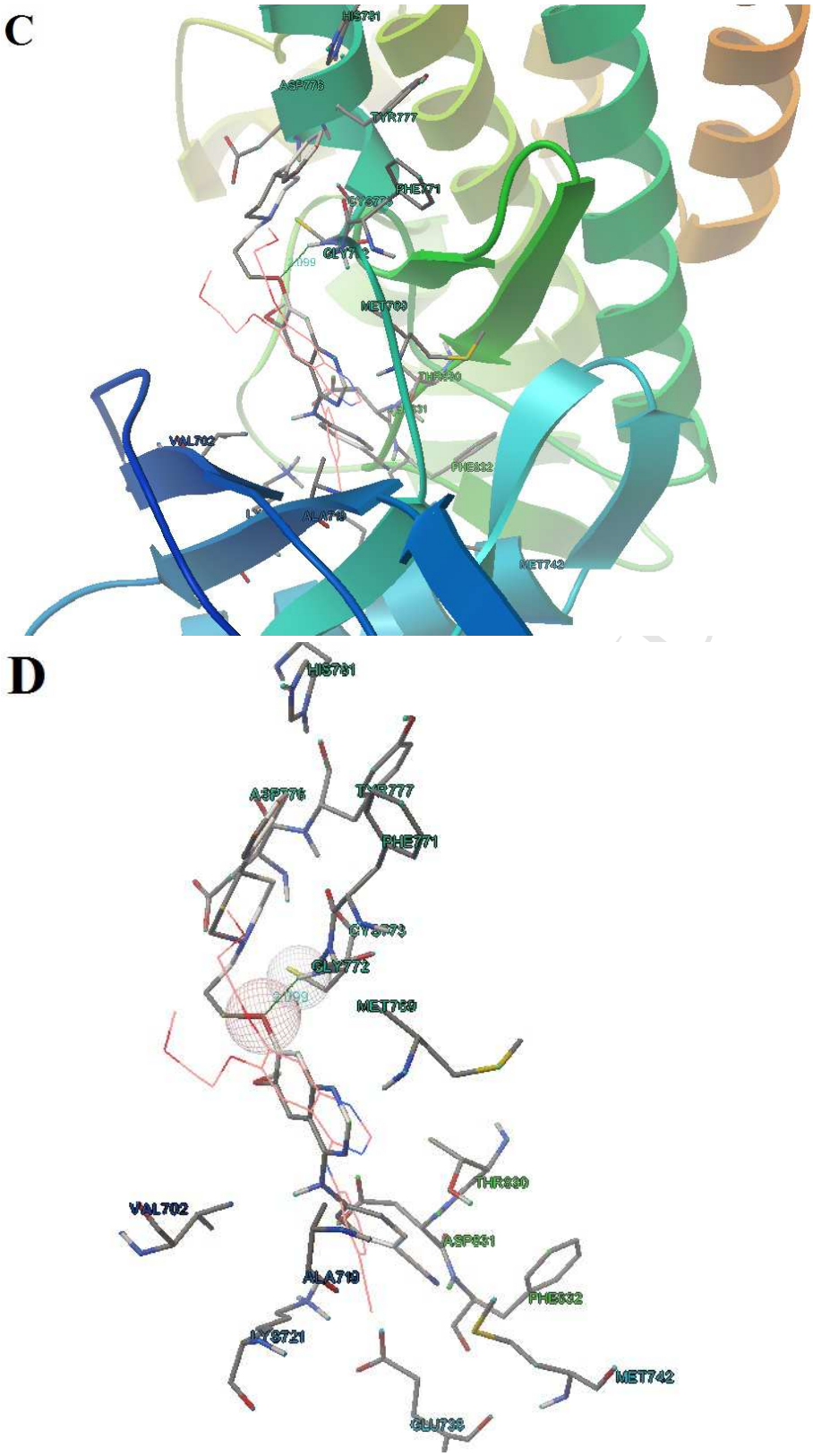

Fig.4 Molecular docking model of compound **21** interacting with EGFR-TK provided by Autodock 4.2.6. A) and B) compound **21** with the ATP binding site of EGFR-TK when benzene ring in the side chain in the axial position, which binding energy is -9.06; C) and D) compound **21** with the ATP binding site of EGFR-TK when benzene ring in the side chain in the equatorial position, which binding energy is -9.22.

Erlotinib is used as a reference.

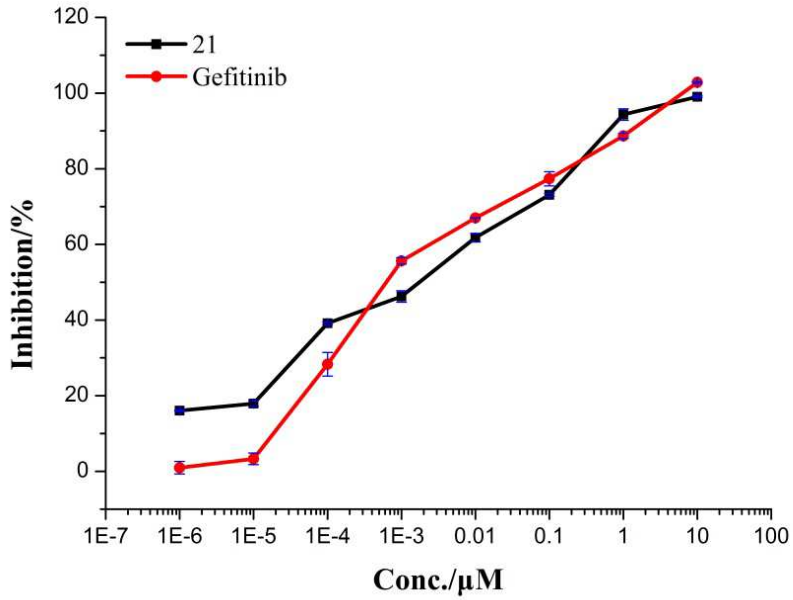

Fig. 5 The concentration-dependent inhibition curves of compound **21** and Gefitinib for EGFR-TK. Points are expressed as mean ± SD of triplicate determinations.

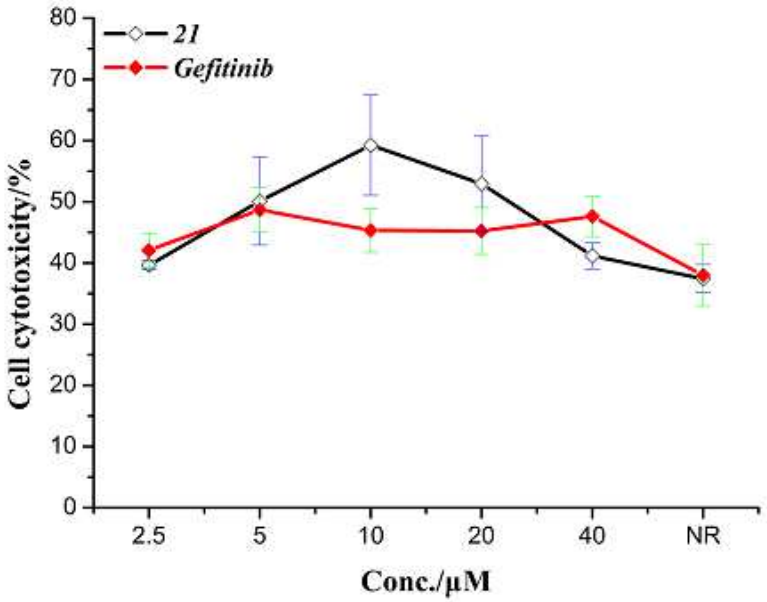

Fig.6 Dose-response cell cytotoxicity curves of tested compounds in HepG2 cells by LDH release at varying concentrations for 48 h. Points are expressed as mean ± SD of triplicate determinations.

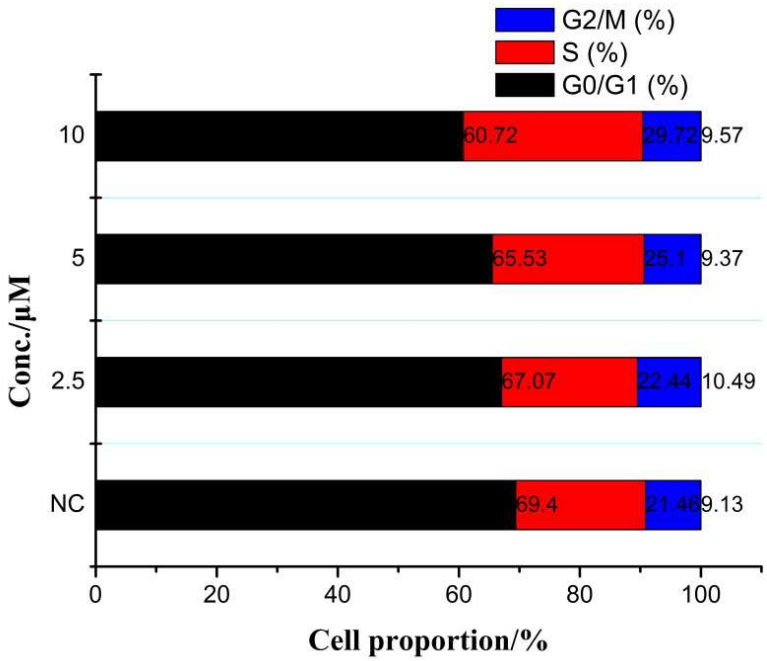

Fig. 7 Statistical results of cell cycle distribution of HepG2 cells treated at varying concentrations of compound **21** for 48 h. The data are present as the average of three independent experiments.

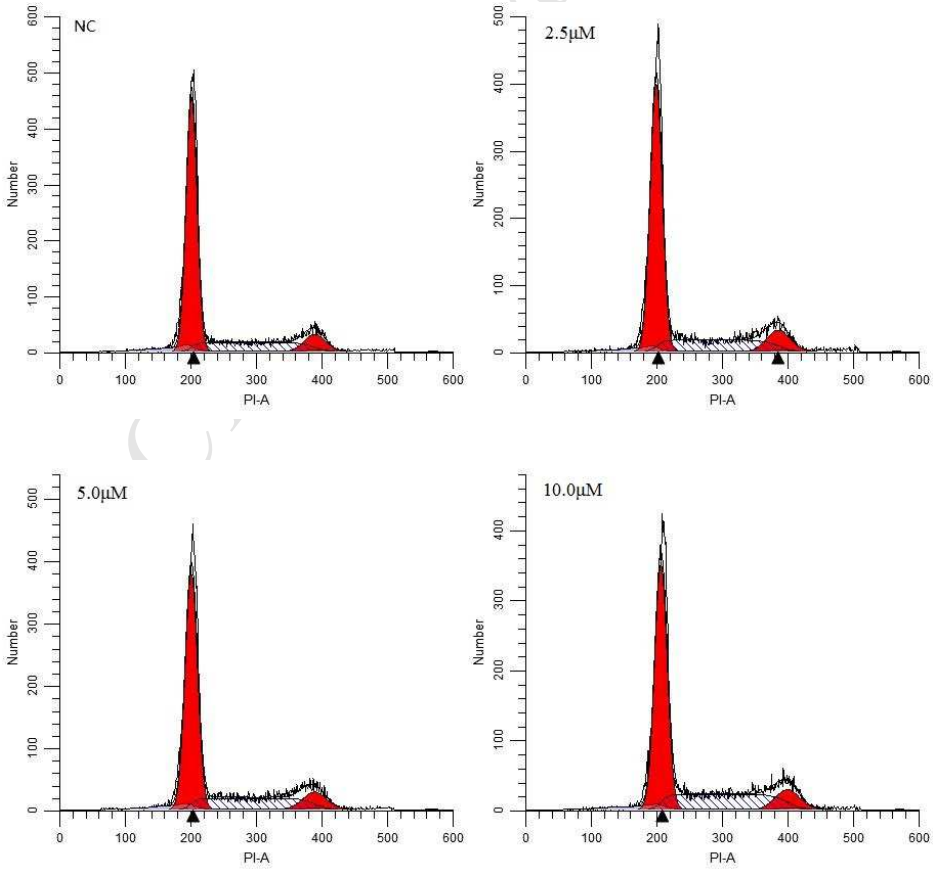

Fig. 8 Cell cycle distribution of HepG2 cells treated at varying concentrations of

compound **21** for 48 h detected by FCM.

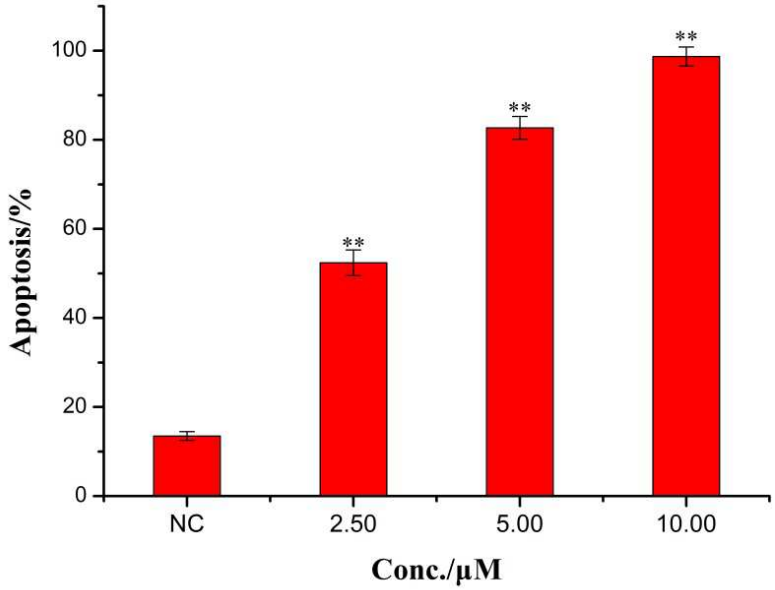

Fig. 9 Statistical results of apoptotic rates of HepG2 cells treated by compound **21** at indicated concentrations. Compared with negative control $^{**}P < 0.01$.

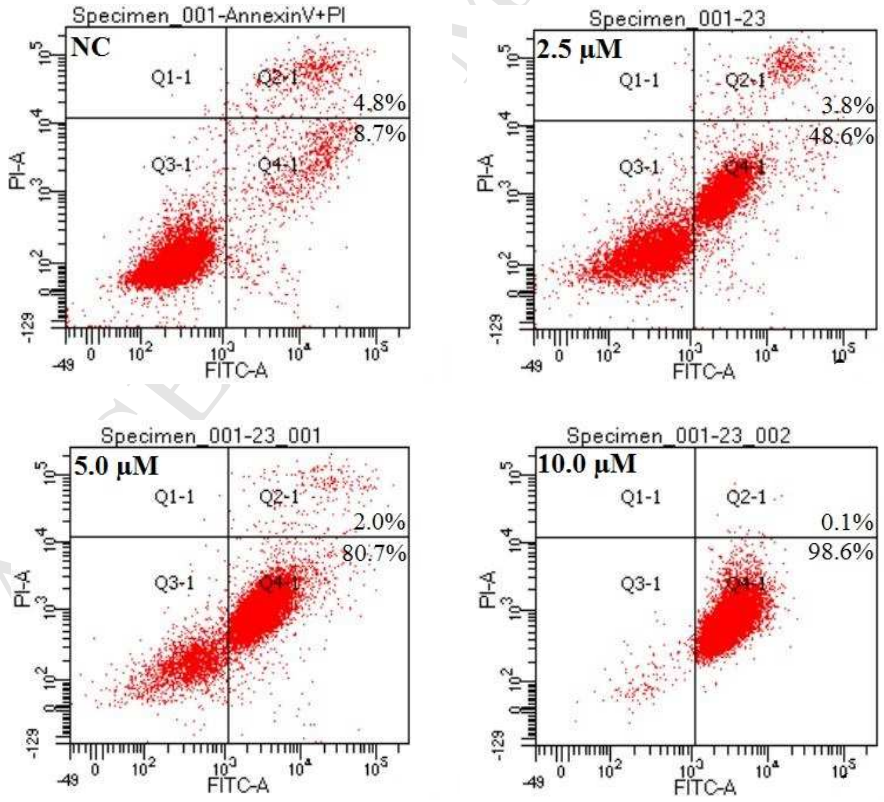

Fig. 10 Cell apoptosis analysis on HepG2 cells treated with compound **21** at indicated concentrations detected by FCM.

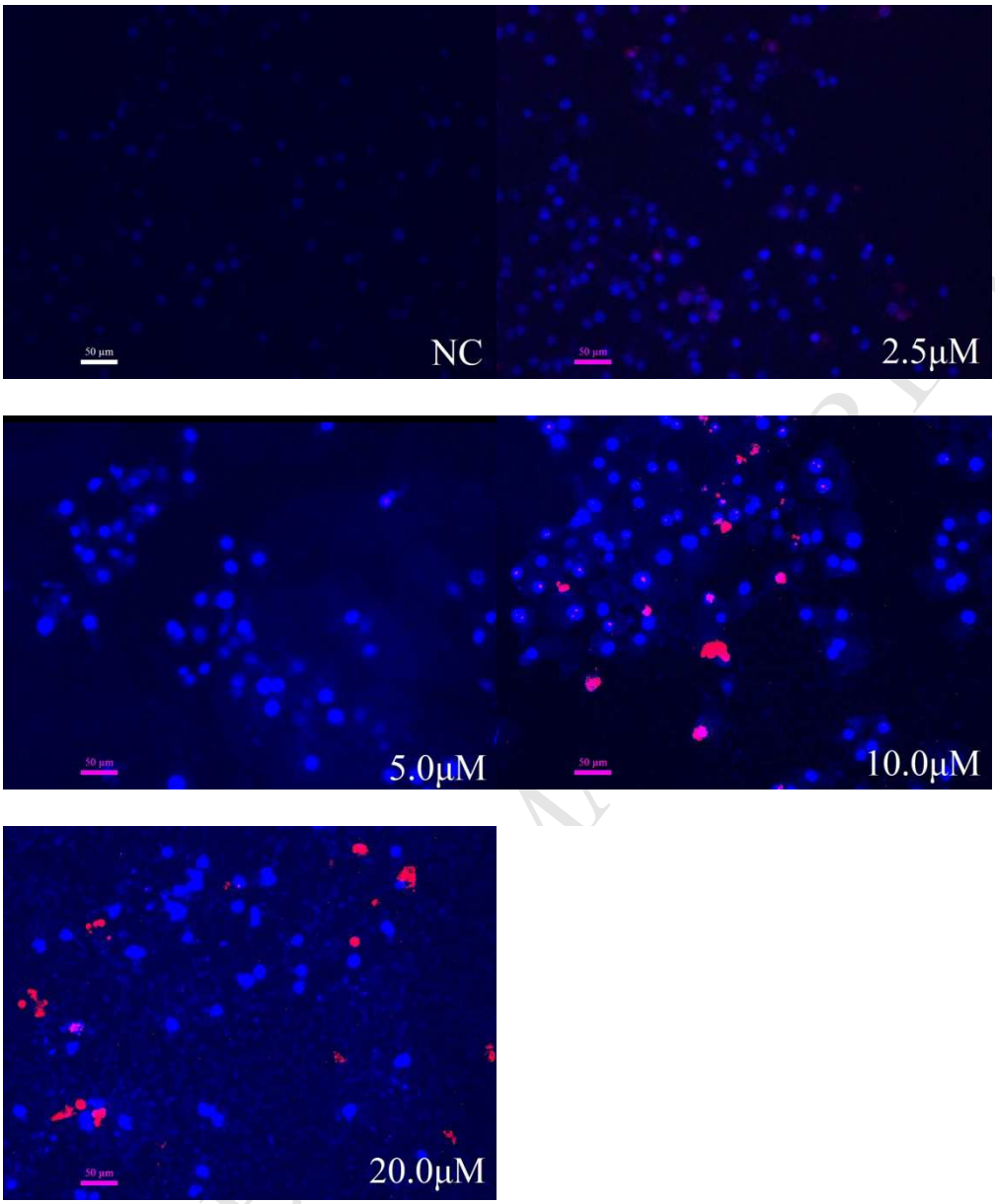

Fig. 11 Morphological observation of HepG2 cells with Hoechst 33342/PI double staining by fluorescence microscope for 48 h (200×).

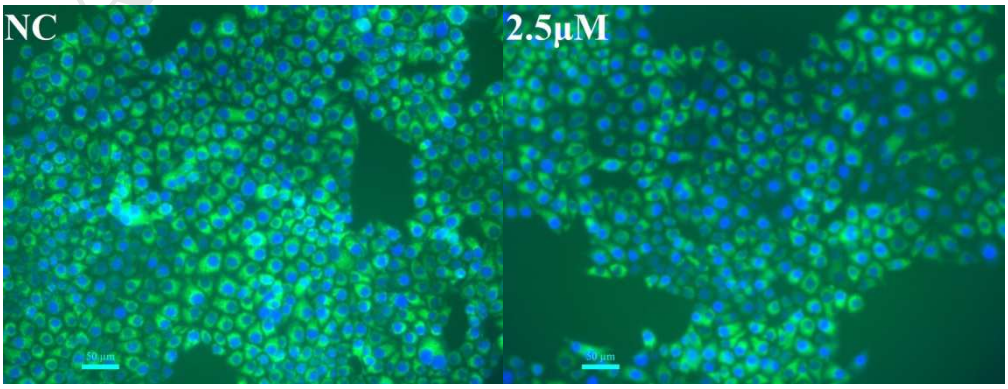

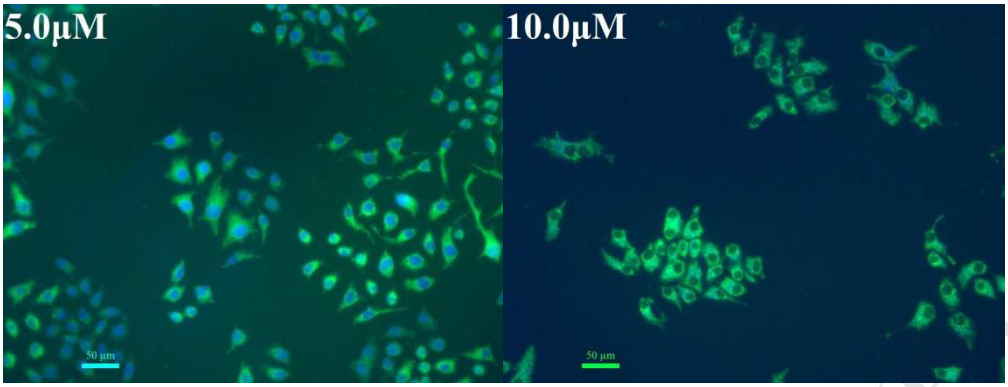

Fig. 12 The changes of mitochondrial membrane potential in HepG2 cells observed by fluorescence microscopy for 48 h (200×).

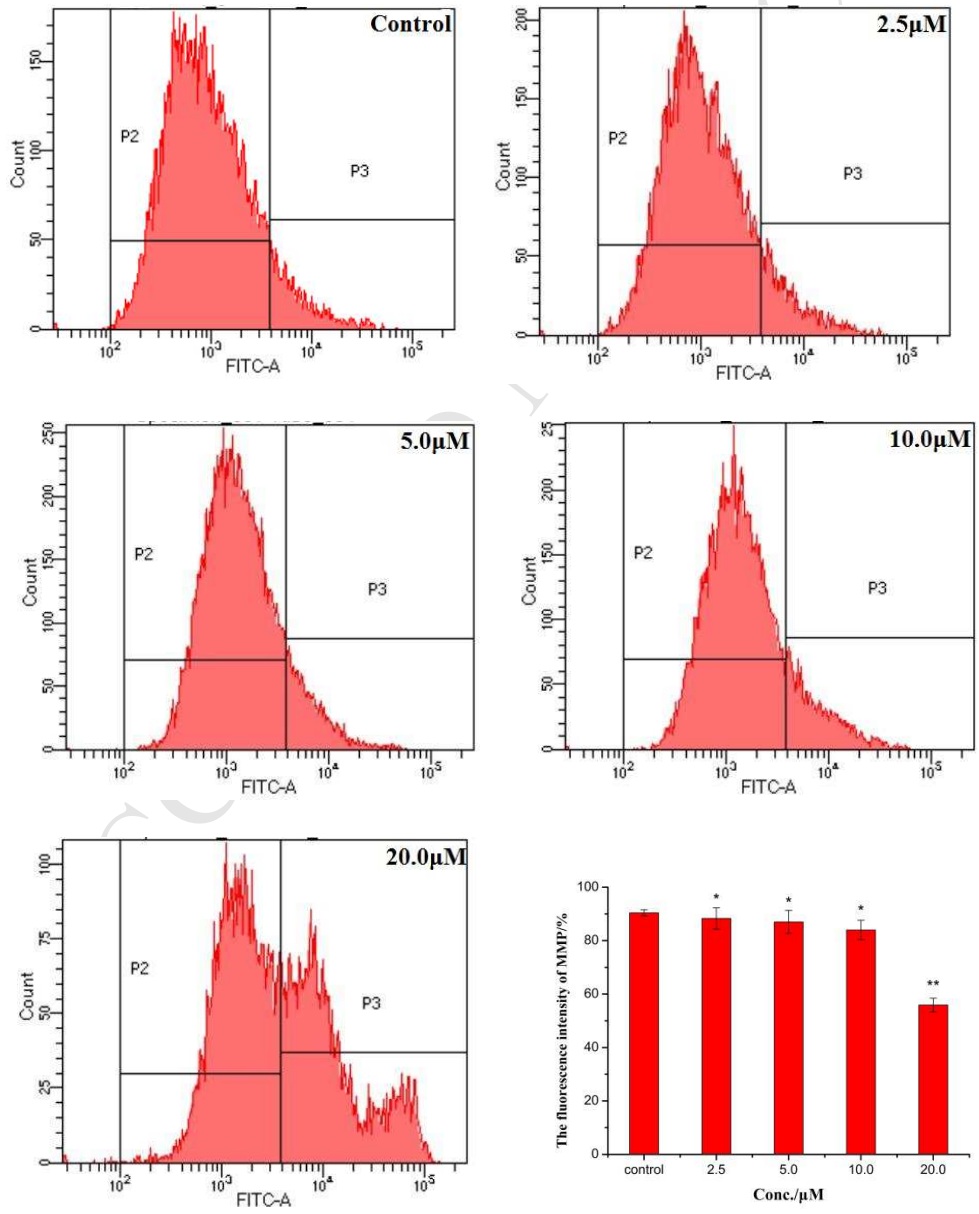

Fig. 13 The changes of mitochondrial membrane potential in HepG2 cells for 48 h

exposure to compound **21** detected by FCM. Data are representative of one of three similar experiments at different time period. Significant differences are indicated by $^{*}P < 0.05$, $^{**}P < 0.01$*vs* negative control group.

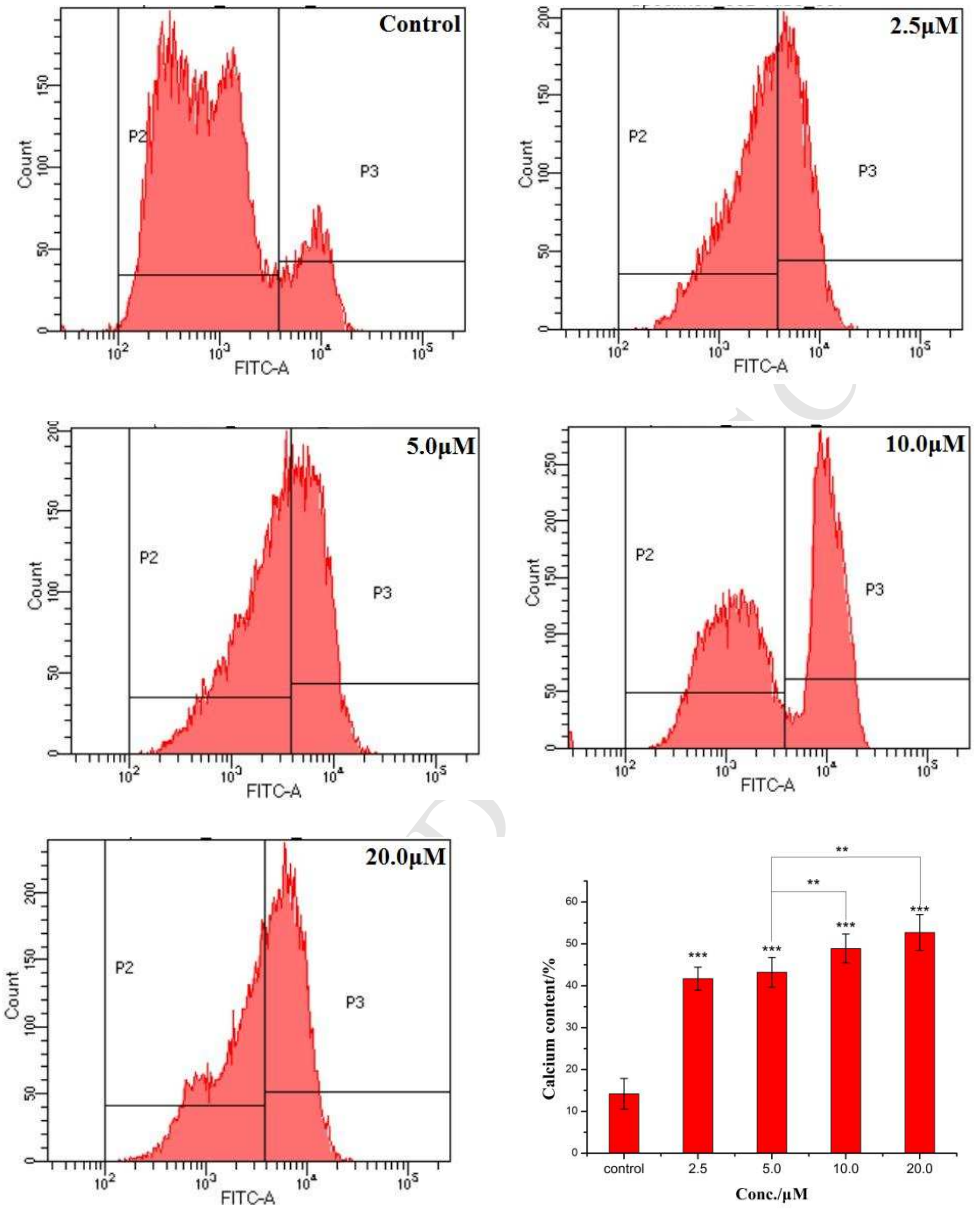

Fig. 14 The changes of intracellular calcium level in HepG2 cells for 48 h exposure to compound **21**. Data are representative of one of three similar experiments at different time period. Significant differences between groups are indicated by $^{**}P < 0.01$, $^{***}P < 0.001$ *vs* negative control group.

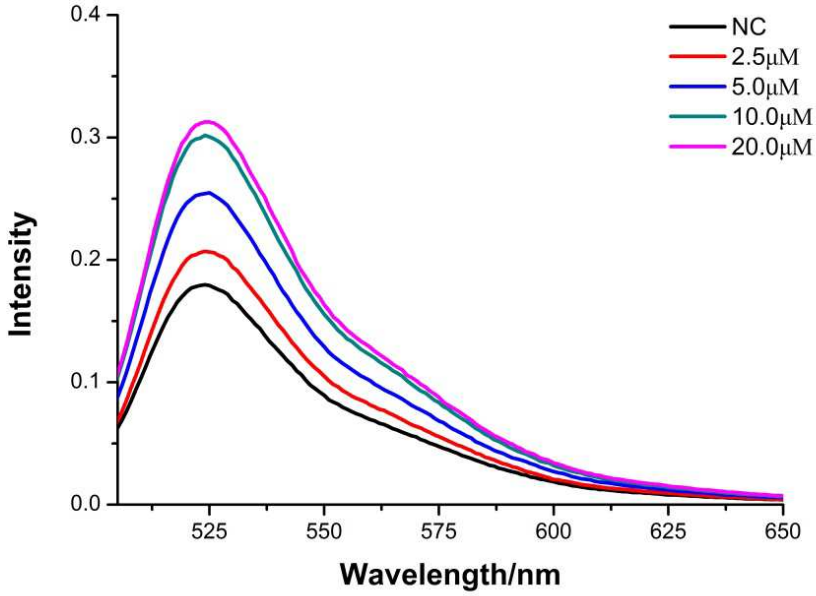

Fig. 15 ROS florescence intensity of HepG2 cells treated with various concentrations of compound **21** for 48 h.

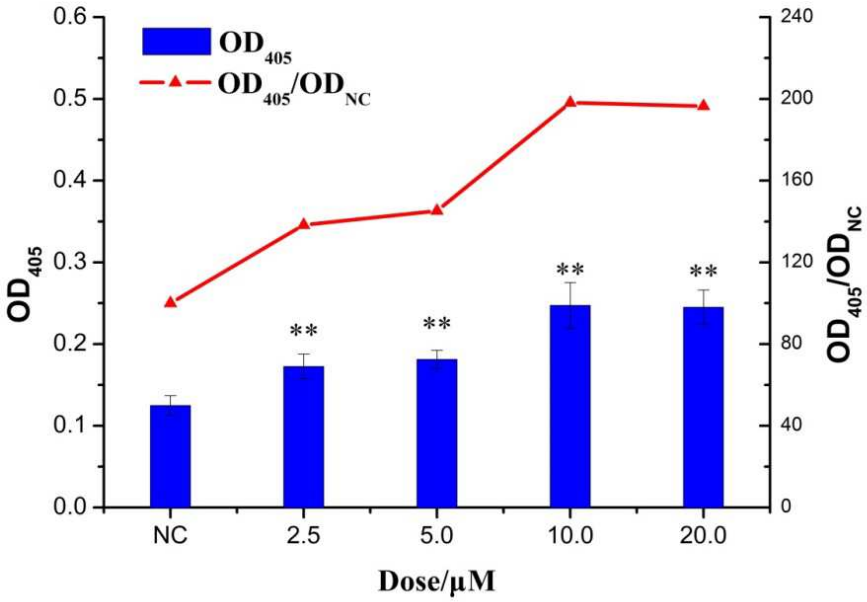

Fig. 16 The activities of caspase-3 in HepG2 cells treated with various concentrations of compound **21** for 48 h. Significant differences between groups are indicated by $^{**}P < 0.01$ vs negative control group.

ACCEPTED MANUSCRIPT

Highlights

- Novel heterocyclic substituted 4-anilinoquinazoline derivatives were designed and synthesized.
- Compound **21** showed better anti-proliferative activity against HepG2 cells than Gefitinib.
- Compound **21** exhibited more potent inhibition in EGFR-TK assay.
- Cytotoxicity of compound **21** against HepG2 cells was investigated.
- Cell cycle, cell apoptosis assays and mechanism of apoptosis were performed.

ACCEPTED MANUSCRIPT